

**University of Alberta**

**Study on Adsorption of Inorganic-organic Hybrid Polymers and  
Flocculation of Oil Sands Tailings**

by

**Shiqing Wang**

A thesis submitted to the Faculty of Graduate Studies and Research  
in partial fulfillment of the requirements for the degree of

**Master of Science**  
in  
**Chemical Engineering**

**Department of Chemical and Materials Engineering**

©Shiqing Wang  
Spring 2013  
Edmonton, Alberta

Permission is hereby granted to the University of Alberta Libraries to reproduce single copies of this thesis and to lend or sell such copies for private, scholarly or scientific research purposes only. Where the thesis is converted to, or otherwise made available in digital form, the University of Alberta will advise potential users of the thesis of these terms.

The author reserves all other publication and other rights in association with the copyright in the thesis and, except as herein before provided, neither the thesis nor any substantial portion thereof may be printed or otherwise reproduced in any material form whatsoever without the author's prior written permission.

## Abstract

Two inorganic-organic hybrid polymers, Al(OH)<sub>3</sub>-polyacrylamide (Al-PAM) and Fe(OH)<sub>3</sub>-polyacrylamide (Fe-PAM) were synthesized and used in flocculating model tailings (5 wt% kaolin suspensions) and laboratory extraction tailings. For comparison, a commercial anionic flocculant, partially hydrolyzed polyacrylamide or Magnafloc 1011 (MF 1011), was also examined. Moreover, a fundamental understanding on flocculation dynamics of model and laboratory extraction tailings by different polymers as well as adsorption kinetics of these polymers on different surfaces was established using focused beam reflectance measurement (FBRM) and quartz crystal microbalance with dissipation (QCM-D), respectively.

For model tailings, Al-PAM, Fe-PAM and MF 1011 exhibited excellent flocculation efficiency, but MF 1011 was found to be sensitive to overdosing. For laboratory extraction tailings, hybrid polymers showed better flocculation performance than MF 1011. Adsorption measurement of polymers by QCM-D indicated that Fe-PAM adsorbed more significantly on bitumen than Al-PAM. Thus, with the presence of bitumen, Fe-PAM could be a better flocculant than Al-PAM in the treatment of oil sands tailings.

## **Acknowledgement**

I would like to thank my supervisor Dr. Zhenghe Xu for his excellent guidance and encouragement throughout my research and graduate studies. I am grateful for the wonderful opportunity he offered me to join the Oil Sands Research Group. His professional attitude and passion for academics inspired me in many ways.

I also would like to thank Dr. Lana Alagha and Dr. Shengqun Wang for their generous help and insightful discussions throughout my project. I appreciate the support and encouragement from members in the Oil Sands Research Group. I wish to especially thank Mr. Haipeng Li for his help in my lab work and presentation. I wish to thank Ms. Yuanchun Hu for providing the procedure of Fe-PAM synthesis; thank Mr. David Yeung and Mr. Aditya Kaura for the preparation of Al-PAM. My appreciation also goes to Mr. Jim Skwarok, Ms. Jie Ru and Ms. Lisa Carreiro for their kind assistance during this work.

The financial support from NSERC Industrial Research Chair in Oil Sands Engineering is also gratefully appreciated.

Finally, my deepest gratitude goes to my parents and my grandparents for their endless love and support. To them I dedicate this thesis.

# Table of Contents

<b>Chapter 1 Introduction.....</b>	<b>1</b>
References.....	5
<b>Chapter 2 Literature Review .....</b>	<b>9</b>
2.1 Generation of Oil Sands Tailings and Management Challenges .....	9
2.2 Current Commercial Tailings Treatment Technologies .....	12
2.2.1 Composite Tailings (CT) .....	12
2.2.2 Thickened Tailings (TT).....	14
2.3 Research on Inorganic-organic Hybrid Polymers.....	16
References.....	18
<b>Chapter 3 Materials and Methodology .....</b>	<b>23</b>
3.1 Materials .....	23
3.1.1 Polymers .....	23
3.1.2 Other Chemicals .....	23
3.1.3 Preparation of Model Tailings .....	24
3.1.4 Preparation of Laboratory Extraction Tailings .....	25
3.2 Settling Test of Model and Laboratory Extraction Tailings .....	27
3.3 Flocculation Test Monitored by FBRM.....	27
3.4 Zeta Potential Measurement .....	28
3.4.1 Model Tailings (Kaolin Suspensions) .....	28
3.4.2 Laboratory Extraction Tailings.....	29
3.5 Measurement of Total Organic Carbon (TOC).....	29

3.6 Adsorption Test Monitored by QCM-D .....	30
3.6.1 Preparation of Bitumen Surfaces for QCM-D Experiment .....	30
3.6.2 QCM-D Experiment .....	31
References.....	32

## **Chapter 4 Synthesis and Characterization of Inorganic-organic Hybrid**

<b>Polymers.....</b>	<b>34</b>
4.1 Materials .....	34
4.2 Synthesis of Inorganic-organic Hybrid Polymers.....	34
4.2.1 Synthesis of Al-PAM.....	34
4.2.2 Synthesis of Fe-PAM.....	35
4.2.3 Purification of Al-PAM and Fe-PAM .....	36
4.3 Characterization of Al-PAM and Fe-PAM .....	36
4.3.1 Molecular Weight .....	36
4.3.2 Metal Content .....	37
References.....	38

## **Chapter 5 Flocculation of Model Tailings .....**

5.1 Effect of Al-PAM on Flocculation .....	40
5.2 Effect of Fe-PAM on Flocculation .....	42
5.3 Effect of MF 1011 on Flocculation.....	43
5.4 Comparison among Al-PAM, Fe-PAM and MF 1011 .....	44
5.5 Strength of Floccs Formed by Different Polymers.....	45
5.6 Effect of Mixing Method on Flocculation .....	46
5.7 Effect of Stirring Rate on Flocculation.....	47

5.8 Summary .....	48
References.....	49
<b>Chapter 6 Adsorption of Polymers on Model Tailings.....</b>	<b>50</b>
6.1 Interaction of Polymers with Model Tailings .....	50
6.2 Adsorption of Polymers on Kaolin Particles .....	52
6.3 Summary .....	53
References.....	55
<b>Chapter 7 Flocculation of Laboratory Extraction Tailings .....</b>	<b>56</b>
7.1 Effect of Al-PAM on Flocculation .....	56
7.2 Effect of Fe-PAM on Flocculation .....	58
7.3 Effect of MF 1011 on Flocculation.....	60
7.4 Comparison among Al-PAM, Fe-PAM and MF 1011 .....	62
7.5 Strength of Flocs Formed by Different Polymers.....	63
7.6 Summary .....	66
References.....	66
<b>Chapter 8 Adsorption of Polymers on Oil Sands Components .....</b>	<b>68</b>
8.1 Interactions of Polymers with Fines in Laboratory Extraction Tailings..	68
8.2 Interactions of Polymers with Bitumen .....	70
8.3 Adsorption of Polymers on Silica (Simulating Silica Basal Planes) .....	71
8.4 Adsorption of Polymers on Alumina (Simulating Alumina Basal Planes) .....	73
8.5 Adsorption of Polymers on Bitumen .....	74

8.6 Comparison among Equilibrium Mass of Polymers Adsorbed on Different Surfaces.....	75
8.7 Summary.....	76
References.....	78
<b>Chapter 9 Conclusions.....</b>	<b>79</b>
<b>Chapter 10 Recommendations for Future Research .....</b>	<b>81</b>

## **List of Tables**

Table 3-1 Characteristics of Polymers Used in This Work .....	23
Table 3-2 Average Concentration of Major Ion in Syncrude Process Water .....	24
Table 3-3 Average Compositon of Laboratory Extraction Tailings .....	26
Table 4-1 Characteristics of Al-PAM and Fe-PAM .....	38

## List of Figures

Figure 2-1 Process Flow Diagram for Water-based Oil Sands Extraction (Shell Canada Muskeg River Operation).....	10
Figure 2-2 Schematic Flow Chart of Composite Tailings Process (Syncrude Canada) .....	13
Figure 3-1 Cumulative Particle Size Distribution of Model Tailings.....	25
Figure 3-2 Cumulative Particle Size Distribution of Laboratory Extraction Tailings.....	26
Figure 5-1 Particle Size Evolution of Model Tailings after the Addition of 10 ppm Al-PAM.....	41
Figure 5-2 Effect of Al-PAM Dosage on Maximum $d_{50}$ of Model Tailings .....	42
Figure 5-3 Effect of Fe-PAM Dosage on Maximum $d_{50}$ of Model Tailings .....	43
Figure 5-4 Effect of MF 1011 Dosage on Maximum $d_{50}$ of Model Tailings.....	43
Figure 5-5 Comparison among Al-PAM, Fe-PAM and MF 1011 .....	44
Figure 5-6 $d_{50}$ of Model Tailings with Polymer Addition as a Function of Time	46
Figure 5-7 Effect of Mixing Method on Flocculation (a) Stirring at 400 rpm without Baffle; (b) Stirring at 400 rpm with Baffle .....	47
Figure 5-8 Effect of Stirring Rate on Flocculation (a) Stirring at 400 rpm; (b) Stirring at 650 rpm .....	48
Figure 6-1 Effect of Polymers on Zeta Potential of Kaolin Particles .....	50
Figure 6-2 Polymer Adsorbed on Kaolin as a Function of Dosage .....	52

Figure 7-1 Effect of Al-PAM Dosage on Maximum $d_{50}$ of Laboratory Extraction Tailings.....	57
Figure 7-2 Comparison between Effect of Al-PAM on Model Tailings and Laboratory Extraction Tailings .....	58
Figure 7-3 Effect of Fe-PAM Dosage on Maximum $d_{50}$ of Laboratory Extraction Tailings.....	58
Figure 7-4 Comparison between Effect of Fe-PAM on Model Tailings and Laboratory Extraction Tailings .....	59
Figure 7-5 Effect of MF 1011 Dosage on Maximum $d_{50}$ of Laboratory Extraction Tailings.....	60
Figure 7-6 Comparison between Effect of MF 1011 on Model Tailings and Laboratory Extraction Tailings .....	61
Figure 7-7 Comparison among Al-PAM, Fe-PAM and MF 1011 .....	63
Figure 7-8 $d_{50}$ of Laboratory Extraction Tailings with Polymer Addition as a Function of Time.....	64
Figure 7-9 Initial Settling Rate of Laboratory Extraction Tailings at Extended Mixing Time .....	65
Figure 8-1 Effect of Polymers on Surface Charge of Fines .....	69
Figure 8-2 Comparison between Effect of Polymers on Surface Charge of Fines in Laboratory Extraction Tailings and Kaolin in Model Tailings .....	70
Figure 8-3 Effect of Polymers on Surface Charge of Bitumen.....	71
Figure 8-4 Adsorption of Polymers on Silica .....	72
Figure 8-5 Adsorption of Polymers on Alumina .....	73

Figure 8-6 Adsorption of Polymers on Bitumen..... 74

Figure 8-7 Comparison among Equilibrium Mass of Polymers Adsorbed on  
Different Surfaces ..... 75

## List of Nomenclature

### Abbreviations

Al-PAM	Al(OH) <sub>3</sub> -polyacrylamide
CHWE	Clark Hot Water Extraction
CT	Composite Tailings
DDA	Dedicated Disposal Area
ERCB	Energy and Resources Conservation Board
Fe-PAM	Fe(OH) <sub>3</sub> -polyacrylamide
FBRM	Focused Beam Reflectance Measurement
ISR	Initial Settling Rate
MF 1011	Magnafloc 1011
MFT	Mature Fine Tailings
NST	Non-segregating Tailings
PAM	Polyacrylamide
PSC	Primary Separation Cell
PSV	Primary Separation Vessel
QCM-D	Quartz Crystal Microbalance with Dissipation
SFR	Sand to Fines Ratio
SMFS	Single Molecule Force Spectroscopy
TT	Thickened Tailings

## Chapter 1 Introduction

The Athabasca area in northern Alberta possesses the largest oil sands deposits in the world. To extract bitumen from the oil sands, the Clark Hot Water Extraction (CHWE) technology has been widely used in the industry. In this process, the oil sands ores are mined, crushed and mixed with warm water. The formed slurry is then transferred to a primary separation vessel (PSV), where bitumen floatation takes place and bitumen is recovered as bitumen froth. The remainder of the slurry, referred to as tailings, is discharged into tailings ponds [1]. The oil sands tailings are warm aqueous suspensions of sands, clays, silts and residual bitumen. In tailings ponds, coarse solids settle to the bottom very rapidly, but much of the fine solids and residual bitumen remain suspended above the sediments. After two to three years of settling, the concentration of suspended fine solids reaches 30% by weight. In oil sands industry, this sludge material is known as mature fine tailings (MFT). Without any treatment, MFT would take centuries to consolidate [2, 3].

Currently, tailings ponds cover more than 170 square kilometers of Alberta's oil sands region and are predicted to increase to 250 square kilometers by 2020 [4]. With the expansion of oil sands mining operations, the fast accumulation of tailings has been the most difficult challenge for the industry, as it causes serious environmental issues. Several technologies have been developed to reduce tailings inventory, including composite tailings (CT) and paste technology. In CT process, coarse solids are added to gypsum-treated MFT to produce non-segregating

tailings (NST). Gypsum ( $\text{CaSO}_4 \cdot 2\text{H}_2\text{O}$ ) is employed as a common coagulant to facilitate the aggregation of fine particles in the MFT slurry by compressing the electric double layers, thus decreasing the surface charges of the suspended particles. Coarse solids create stress on the aggregated fines to accelerate densification of MFT. Water generated as supernatant is recycled to bitumen extraction plant. However, the use of gypsum as a coagulant in CT technology leads to a significant amount of  $\text{Ca}^{2+}$  ions in the recycled process water, which deteriorates bitumen recovery [5, 6].

Paste technology is one of the most promising practices for oil sands tailings management. In paste technology, synthetic polymers are used to flocculate fine solids and accelerate their settling. As a result, high density, low moisture content thickened tailings can be produced, which offers significant economic incentives and environmental benefits. The performance of flocculants is a key factor in paste technology. Cymerman et al. [5] conducted a series of studies to investigate the efficiency of flocculants with different molecular weights and charge densities. It has been reported that anionic co-polymers of acrylamide and acrylates such as MF 1011, are very effective in flocculating oil sands fine tailings at pH 8.5. The flocculation is induced by formation of hydrogen bonds between polymer chains and fine particles. However, MF 1011 was unable to give a clear aqueous supernatant and was not effective in improving filtration of oil sands tailings [7].

Inorganic-organic hybrid polymers are well-known for their unique structural properties. Integrating inorganic moieties into the polymer architectures is

anticipated to improve their function when used as process aids in a variety of research areas [8-15]. Cationic inorganic-organic hybrid polymer,  $\text{Al}(\text{OH})_3$ -polyacrylamide (Al-PAM) is known to be effective when used in flocculating both kaolin suspensions and oil sands tailings. Al-PAM was able to induce the formation of larger and denser flocs compared to open flocs structure obtained by the addition of commercial polyacrylamide (PAM) and the PAM/ $\text{AlCl}_3$  blend [15]. When used as filtration aids, Al-PAM has also been demonstrated to form very dry filter cakes [3]. The enhanced flocculation performance could be attributed to two synergistic processes: positively charged  $\text{Al}(\text{OH})_3$  colloids adsorb on the surfaces of negatively charged clay particles through charge neutralization mechanism, thus reducing the particle-particle repulsion to bring particles in close proximity to facilitate effective bridging by PAM chains [16]. Alagha et al. studied the adsorption kinetics of Al-PAM and MF 1011 on silica (simulating silica basal planes) and alumina (simulating alumina basal planes) surfaces using quartz crystal microbalance with dissipation (QCM-D). The results indicated that Al-PAM has a higher affinity to silica surfaces than to alumina surfaces, while MF 1011 exhibits strong adsorption on alumina but negligible adsorption on silica [16].

Recently, another novel inorganic-organic hybrid polymer,  $\text{Fe}(\text{OH})_3$ -polyacrylamide (Fe-PAM) was synthesized and found to be as effective as Al-PAM in flocculating both kaolin suspensions and laboratory extraction oil sands tailings. Moreover, Fe-PAM is shown to be more efficient than Al-PAM in the filtration of laboratory extraction oil sands tailings [17]. This difference in

performance is attributed to the significant adsorption of Fe-PAM on bitumen that remains in the tailings slurry, although in small quantities, after the extraction process, leading to effective co-flocculation of fine solids with fine bitumen droplets. The effective co-flocculation of fine bitumen droplets and fine solids prevents blinding of filter medium and pores of filter cake, accelerating the filtration process and leading to cleaner filter medium [17]. However, fundamental understanding on the adsorption kinetics of Fe-PAM at solid-liquid interfaces as well as tailings flocculation dynamics has not been investigated yet.

Focused beam reflectance measurement (FBRM) provides an in-situ real-time analysis of particle size in suspensions or emulsions. FBRM has already been used in studying the flocculation processes of microcrystalline cellulose, pulp suspension, marine microalgae, etc [18-22]. During the measurement, a laser beam is generated in the FBRM probe, fixed on the edge of a high speed rotator and focused into the dispersion medium. When the laser beam hits the surface of a particle, some of the light will be reflected back into the probe. The duration of this reflected pulse is converted to the chord length of the particle [18, 19].

In the present work, focused beam reflectance measurement (FBRM) and quartz crystal microbalance with dissipation (QCM-D) were used to study the flocculation dynamics and adsorption kinetics of cationic hybrid polymers: Al-PAM and Fe-PAM on solid surfaces. The floc size and stability of kaolin suspensions and laboratory extraction oil sands tailings were systematically studied under different polymer dosages and shear rates using FBRM. Once the optimum flocculation dosage of each polymer was obtained, QCM-D tests were

conducted to determine the adsorption of polymers at their optimum dosages on silica, alumina and bitumen surfaces. Process water was used in both flocculation and adsorption experiments for better understanding of the role of polymers in the two processes.

This thesis is divided into 10 chapters: Chapter 1, Introduction; Chapter 2, Literature Review; Chapter 3, Materials and Methodology; Chapter 4, Synthesis and Characterization of Inorganic-organic Hybrid Polymers; Chapter 5, Flocculation of Model Tailings; Chapter 6, Adsorption of Polymers on Model Tailings; Chapter 7, Flocculation of Laboratory Extraction Tailings; Chapter 8, Adsorption of Polymers on Oil Sands Components; Chapter 9, Conclusions; and Chapter 10, Recommendations for Future Research.

## References

1. Li, H.; Long, J.; Xu, Z.; Masliyah, J. H. Novel polymer aids for low-grade oil sand ore processing. *The Canadian Journal of Chemical Engineering* **2008**, *86* (2), 168-176.
2. Zhu, R.; Liu, Q.; Xu, Z.; Masliyah, J. H.; Khan, A. Role of dissolving carbon dioxide in densification of oil sands tailings. *Energy and Fuels* **2011**, *25* (5), 2049-2057.
3. Wang, X. W.; Feng, X.; Xu, Z.; Masliyah, J. H. Polymer aids for settling and filtration of oil sands tailings. *The Canadian Journal of Chemical Engineering* **2010**, *88* (3), 403-410.

4. Simeritsch, T.; Obad, J.; Dyer, S. *Tailings Plan Review*; The Pembina Institute and Water Matter: December 2009.
5. Cymerman, G.; Kwong, T.; Lord, E.; Hamza, H.; Xu, Y. In *Proceedings of the 3rd UBC-McGill Biannual International Symposium on Fundamentals of Mineral Processing*, 1999; 1999; pp 605-619.
6. Li, H.; Long, J.; Xu, Z.; Masliyah, J. H. Flocculation of kaolinite clay suspensions using a temperature-sensitive polymer. *AIChE Journal* **2007**, *53* (2), 479-488.
7. Wang, X. Polymer Aids for Settling and Filtration of Oil Sands Tailings. MSc Thesis, University of Alberta, Edmonton, 2010.
8. Chujo, Y. Organic-inorganic hybrid materials. *Solid State & Materials Science* **1996**, *1*, 806-811.
9. Wei, Y.; Jin, D.; Yang, D.; Xu, J. Novel organic-inorganic chemical hybrid filters for dental composite materials. *Journal of Applied Polymer Science* **1998**, *70*, 1689-1699.
10. Novak, B. M. Hybrid nanocomposite materials-between inorganic glasses and organic polymers. *Advanced Materials* **1993**, *5* (6), 422-433.
11. Yano, S.; Iwata, K.; Kurita, K. Physical properties and structure of organic-inorganic hybrid materials produced by sol-gel process. *Materials Science and Engineering C* **1998**, *6*, 75-90.
12. Seddon, A. B. Sol-gel derived organic-inorganic hybrid materials for photobic applications. *IEE Proceedings: Circuits, Devices and Systems* **1998**, *145* (5), 369-372.

13. Ahmed, Z.; Mark, J. E. Biominetic materials: recent development in organic-inorganic hybrids. *Materials Science and Engineering C* **1998**, *6*, 183-196.
14. Ye, H.; Zhao, J. Q.; Zhang, Y. H. Novel degradable superabsorbent materials of silicate/acrylic-base polymer hybrids. *Journal of Applied Polymer Science* **2004**, *91*, 936-940.
15. Yang, W. Y.; Qian, J. W.; Shen, Z. Q. A novel flocculant of Al(OH)<sub>3</sub>-polyacrylamide ionic hybrid. *The Journal of Colloid and Interface Science* **2004**, *273* (2), 400-405.
16. Alagha, L.; Wang, S.; Xu, Z.; Masliyah, J. Adsorption Kinetics of a Novel Organic-Inorganic Hybrid Polymer on Silica and Alumina Studied by Quartz Crystal Microbalance. *Journal of Physical Chemistry C* **2011**, *115* (31), 15390-15402.
17. Hu, Y. A Novel Fe-PAM Flocculant for Oil Sands Tailings Treatment. Oil Sands Research Group Student Presentation, Syncrude Research Centre, Edmonton, 2011.
18. Alfano, J. C.; Carter, P. W.; Dunham, A. J.; Nowak, M. J.; Tubergen, K. R. Polyelectrolyte-induced aggregation of microcrystalline cellulose: Reversibility and shear effects. *Journal of Colloid and Interface Science* **2000**, *223* (2), 244-254.
19. Blanco, A.; Fuente, E.; Monte, M. C.; Cortés, N.; Negro, C. Polymeric branched flocculant effect on the flocculation process of pulp suspensions

- in the papermaking industry. *Industrial and Engineering Chemistry Research* **2009**, *48* (10), 4826-4836.
20. Uduman, N.; Qi, Y.; Danquah, M. K.; Hoadley, A. F. A. Marine microalgae flocculation and focused beam reflectance measurement. *Chemical Engineering Journal* **2010**, *162* (3), 935-940.
21. Óciardhá C. T.; Mitchell, N. A.; Hutton, K. W.; Frawley, P. J. Determination of the crystal growth rate of paracetamol as a function of solvent composition. *Industrial and Engineering Chemistry Research* **2012**, *51* (12), 4731-4740.
22. Thapa, K. B.; Qi, Y.; Hoadley, A. F. A. Interaction of polyelectrolyte with digested sewage sludge and lignite in sludge dewatering. *Colloids and Surfaces A: Physicochemical and Engineering Aspects* **2009**, *334* (1-3), 66-73.

## **Chapter 2 Literature Review**

### **2.1 Generation of Oil Sands Tailings and Management Challenges**

Oil sands, as a naturally occurring mixture of sand, clay, water and bitumen, are a type of unconventional oil deposits. Oil sands were found in several locations around the world, including Canada, Venezuela, the United States and Russia. With an estimated 176.8 billion barrels of oil reserves in oil sands, Canada ranked the second only to Saudi Arabia as an oil resource country [1]. The Athabasca deposit in Alberta, northern Canada is the largest and most developed oil sands reservoir in the world [2]. An oil sand ore typically contains 7-14 wt% bitumen, 83-88 wt% mineral solids and 3-5 wt% water [3]. There are two main methods to extract bitumen from oil sands: surface mining for reserve at a depth of less than 75 m and in-situ recovery for oil sands buried at larger depths. It is estimated that 80% of bitumen deposit can be recovered only through in-situ technologies, but currently surface mining is still the major method employed by most oil sands operators for bitumen recovery [4]. A typical flow chart of bitumen extraction from minable oil sands is shown in Figure 2-1.

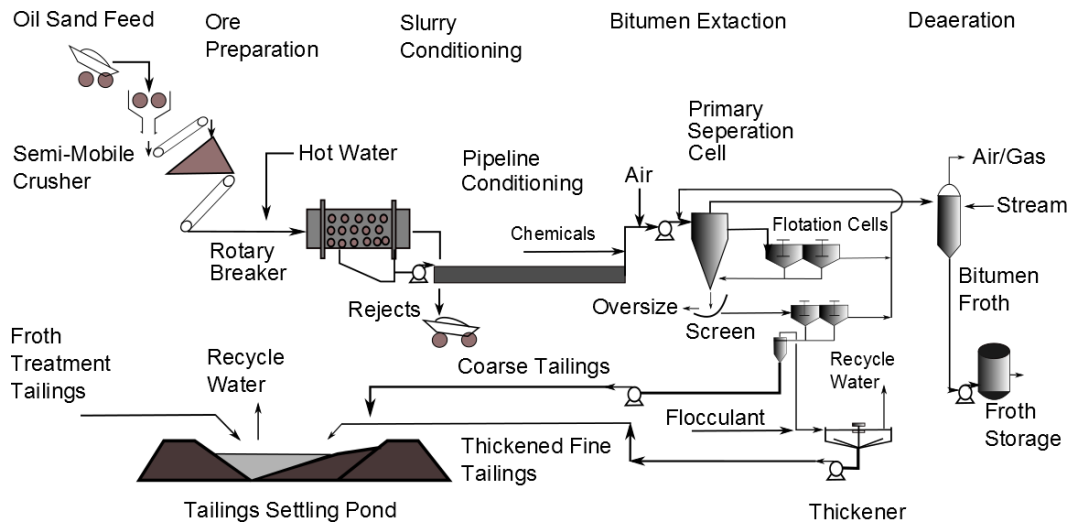


Figure 2-1 Process Flow Diagram for Water-based Oil Sands Extraction  
(Shell Canada Muskeg River Operation) [5]

First, oil sands are mined using shovels and transported by trucks. Then the oil sands ores are crushed into smaller pieces and mixed with warm water and chemical additives. The slurry is transported to a primary separation vessel (PSV) or primary separation cell (PSC) through hydrotransport pipelines [6]. This step involves bitumen liberation and aeration [7]. Separation of the liberated and aerated bitumen from the slurry takes place in PSV or PSC, where a bitumen rich froth containing 60 wt% bitumen, 30 wt% water and 10 wt% solids is recovered. The bitumen froth is then de-aerated, sent to froth treatment unit to produce clean bitumen, which is upgraded into different streams of hydrocarbons [3]. The remainder of the slurry, containing sands, clays, silts and residual bitumen, is discharged into tailings ponds, where coarse solids settle to the bottom rapidly, leaving a clear layer of water for recycle, but much of the fine solids and residual bitumen remain suspended above the sediments. After two to three years, when

the concentration of suspended fine solids reaches 30% by weight, it is referred to as mature fine tailings (MFT) [8]. Without any treatment, MFT would take centuries to consolidate [8, 9].

The accumulation of MFT has been a concern for the oil sands industry for more than four decades [10]. Due to the zero discharge policy, tailings are stored in tailings ponds for settling and consolidation. The tailings ponds now cover more than 170 square kilometers of the northeastern Alberta landscape, which is 50% larger than the city of Vancouver [11]. The unrecovered hydrocarbons are hurting wildlife. In recent years, thousands of ducks have died in tailings ponds in the Fort McMurray area [5]. The environmental issues and pressure on landscape caused by growing volume of tailings ponds make management of oil sands tailings one of the most vexing challenges for the oil sands operators.

Alberta Energy and Resources Conservation Board (ERCB) released Directive 074: Tailings Performance Criteria and Requirements for Oil Sands Mining Schemes. The main purpose of Directive 074 is to regulate the reclamation of tailings. The mineable oil sands operators are accountable for reducing the volume of fluid fine tailings produced during the bitumen extraction process and creating 'trafficable surfaces'. To obtain the 'trafficable surfaces', deposits must have a minimum shear strength. For the material deposited in the previous year, the minimum undrained shear strength should achieve 5 kPa; and within five years, the deposit should have the strength, stability and structure necessary to establish a trafficable surface layer with a minimum undrained shear strength of

10 kPa [12]. Companies have to submit tailings management plans to ERCB to show how they intend to meet the directive's requirements.

## **2.2 Current Commercial Tailings Treatment Technologies**

Several technologies have been developed for dewatering of oil sands tailings, including mechanical processes, natural processes, chemical amendments, bioremediation, etc [13]. Based on their technical and economic feasibility, CT employed by Syncrude Canada Ltd. and thickened tailings (TT) utilized by Shell Canada Ltd. are the most commercially used tailings treatment technologies.

### **2.2.1 Composite Tailings (CT)**

CT technology was developed at the University of Alberta. In this process, densified extraction tailings from cyclone underflow and MFT with a coagulant were mixed to create non-segregating tailings (NST) [3]. The coagulant is typically gypsum ( $\text{CaSO}_4 \cdot 2\text{H}_2\text{O}$ ). Calcium ions from gypsum can lead to the aggregation of clays by compressing the electric double layer and decreasing surface charge [14]. Upon deposition in a tailings pond, the slurry becomes more viscous, then a solid-free water layer was released to the surface and the deposit becomes denser. With subsequent loading of NST layers, more water will be squeezed out and eventually a solid material is formed. The water released from tailings ponds is recycled to the bitumen extraction process. Figure 2-2 shows the schematic of a CT process.

## Composite Tailings Process

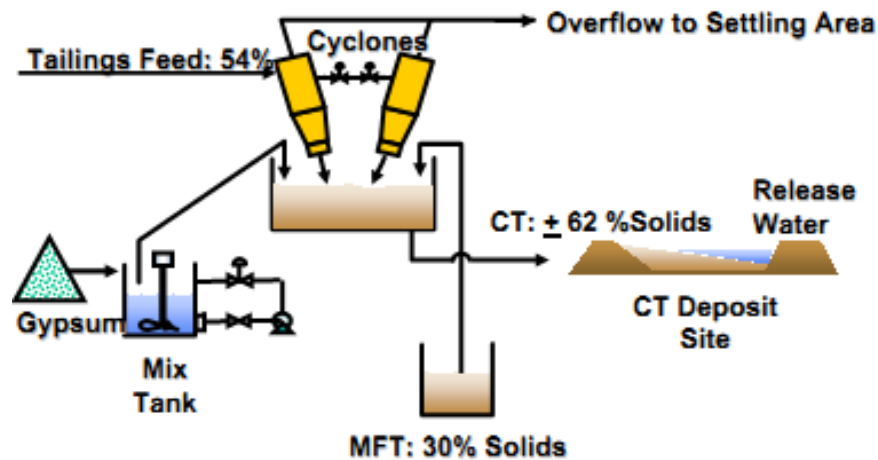


Figure 2-2 Schematic Flow Chart of Composite Tailings Process (Syncrude Canada) [15]

The first important step to create NST is to achieve a proper sand to fines ratio (SFR), because non-segregating characteristics of final slurry is obtained only when the final slurry has a specific percentage of fines in solids [16]. For example, a slurry containing approximately 60% solids in total and 25% fines in solids, is of the non-segregating type. However, slurry with 45% solids in total and less than 20% fines in solids would not form NST. A SFR of 4:1 has been chosen for commercial use through research and development efforts. This SFR will provide adequate geotechnical performance [16].

Another crucial step in CT process is the addition of coagulant, as it changes properties of the clays in CT mixture and thus prevents fines from segregating from the sands when CT is deposited in tailings ponds. Various coagulant aids were tested during the development of the CT process, such as lime (CaO,

Ca(OH)<sub>2</sub>), gypsum (CaSO<sub>4</sub> · 2H<sub>2</sub>O), sodium aluminate (Na<sub>2</sub>Al<sub>2</sub>O<sub>3</sub>), etc. Based on research efforts, gypsum was proven to be a robust and most effective coagulant for commercial applications [3].

The CT technology has been employed by Syncrude Canada Ltd. and Suncor Energy Inc. for nearly two decades. It accelerated tailings densification and reclamation. However, the Ca<sup>2+</sup> and SO<sub>4</sub><sup>2-</sup> ions released to the recycle water were found to be detrimental to bitumen extraction [15, 17]. Also, due to the discharge of warm cyclone overflow water into the tailings pond, the CT process may decrease the thermal energy efficiency of the oil sands operations. In addition, it would potentially cause H<sub>2</sub>S emissions through anaerobic reduction of SO<sub>4</sub><sup>2-</sup> with the un-recovered bitumen in tailings [18]. Moreover, the high salinity of tailings from CT process would harm the boreal forest [19].

### **2.2.2 Thickened Tailings (TT)**

TT technology, also referred to as paste technology, involves rapid settling of the fine portion of fresh tailings within a process vessel, namely thickener, through the addition of synthetic organic chemicals that flocculate the fine solids. Warm water (overflow of the thickener) recovered from the tailings, before they are deposited in storage facilities, is recycled back to the bitumen extraction process with little loss of temperature. The process water requires less make-up heating, which reduces energy use and greenhouse gas emissions. The concentrated stream of fine tailings (underflow of the thickener) will be transferred to the dedicated disposal area (DDA) to help speed up the release of water from the solids [13].

The efficiency of flocculants is of critical importance to TT technology. The most frequently used polymeric flocculants are derived from the acrylamide monomer [20]. The non-ionic polyacrylamide (PAM) is an effective flocculant and its activity can be enhanced by copolymerization with other monomers. This can introduce functional groups to the polymer, which have a high affinity for a particular mineral phase or opposite surface charge from fine particles [21]. MF 1011, an anionic co-polymer of acrylamide and acrylates, is a commercial flocculant used in TT technology. It has a molecular weight of 17.5 million Da and charge density of 22%. Addition of MF 1011 to oil sands fine tailings at pH 8.5 led to the formation of fast settling flocs, but the supernatant still contains 1.5 wt% of solids. MF 1011 binds to suspended fine particles through hydrogen bonding, leading to the formation of heavier flocs that rapidly settle down. Cymerman et al. conducted pilot plant test in a continuous thickener, and they found that upon proper use of MF 1011 and operation, the thickener overflow had less than 0.8 wt% of solids, and the underflow paste had 52-65 wt% of solids [3].

The advantage of TT technology is as follows: first, coarse tailings are easily separated from the mixture, which can be re-used to construct mounds, dikes and other stable deposits; secondly, the produced thickened tailings can be deposited with less land disturbance and may accelerate land reclamation; finally, it is able to substantially reduce or even eliminate the production of new fine tailings, and thus to reduce the size of tailings ponds and expedite recycling of water back to the bitumen extraction process [13].

### 2.3 Research on Inorganic-organic Hybrid Polymers

Inorganic-organic hybrids are attractive materials for creating high performance through the synergism of two components. Their applications range over photochromic films, selective membranes, optical materials, coatings and electrical conducting materials [22-27].

Yang et al. synthesized inorganic-organic hybrid polymer: Al(OH)<sub>3</sub>-polyacrylamide (Al-PAM) with ionic bonds between Al(OH)<sub>3</sub> colloids and PAM chains. They evaluated its effect on flocculation of kaolin suspensions and found that compared with PAM or PAM/AlCl<sub>3</sub> blend, Al-PAM is the most effective in flocculating kaolin suspensions in terms of settling rate. Also, the kaolin flocs induced by Al-PAM was larger, denser and generally have good resistance to shear. They concluded that the high flocculation efficiency of Al-PAM could be attributed to the synergism of two processes: the cationic Al(OH)<sub>3</sub> colloid attracted the negative kaolin particles by electrostatic interaction, and the PAM chains adsorb on kaolin surfaces by hydrogen bonds [28].

Sun et al. studied the Al-PAM induced pelleting flocculation by single molecule force spectroscopy (SMFS). The SMFS results revealed the star-like structure of Al-PAM: Al(OH)<sub>3</sub> colloids cores connecting PAM chains. This kind of structure contributed to the formation of pellet-like flocs and thus enhanced flocculation performance of Al-PAM. Their SMFS results also showed that the positively charged Al(OH)<sub>3</sub> colloid particles strongly attached to the silica surface with an

adhesion force of ~1250 pN, while the adhesion force between PAM chains and the silica surface was only ~250 pN [29].

Wang et al. investigated Al-PAM assisted settling and filtration of model tailings, laboratory extraction tailings and paraffinic froth treatment tailings. For model tailings prepared with kaolin and sand with a SFR of 4, Al-PAM improved their settling rate dramatically. Upon addition of 10 ppm Al-PAM, the initial settling rate (ISR) of model tailings containing 25 wt% solids increased from 0 to over 20 m/h, and the solids content of sediment reached 64 wt%. Al-PAM was also shown to be an effective filtration aid: it lowered the moisture content of model tailings from 50 wt% to less than 20 wt%. For laboratory extraction tailings, 30 ppm Al-PAM was able to increase the ISR from 0 to over 40 m/h. Applying Al-PAM to the filtration of laboratory extraction tailings was also successful: with 10 ppm Al-PAM, the filtration cake only contained around 6 wt% of moisture. In contrast, MF 1011 was found ineffective in filtration of laboratory extraction tailings [8].

Guo et al. conducted research on effect of molecular weight and Al content of Al-PAM on settling and filtration of oil sands tailings. They found that Al-PAM with higher molecular weight and Al content is better for settling and filtration [30].

Alagha et al. studied the adsorption kinetics of Al-PAM with various molecular weights and Al contents on silica and alumina surfaces by QCM-D. They found that Al-PAM showed more rapid adsorption on silica than on alumina. When increasing the molecular weight and aluminum content of Al-PAM, its adsorption

on silica also increased. But Al-PAM with lower aluminum content adsorbed more on alumina [31].

Recently, a novel inorganic-organic hybrid polymer, Fe(OH)<sub>3</sub>-polyacrylamide (Fe-PAM) was synthesized [32] and employed in settling and filtration of kaolin suspensions and laboratory extraction tailings. Fe-PAM was found to be as effective as Al-PAM in flocculation of both model and laboratory extraction tailings. Fe-PAM is slightly more effective than Al-PAM in filtration of laboratory extraction tailings [33]. However, the adsorption kinetics of Fe-PAM at solid-liquid interfaces as well as the flocculation dynamics of model and laboratory extraction tailings with Al-PAM and Fe-PAM have not been investigated yet, which is the subject of this thesis.

## References

1. Attanasi, E.; Meyer, R. *Natural Bitumen and Extra-Heavy Oil*; World Energy Council: 2010; pp 123-140.
2. Syncrude Athabasca Oil Sands Mine, Alberta, Canada.  
<http://www.mining-technology.com/projects/syncrude/>
3. Masliyah, J. H., *Fundamentals of oil sands extraction: CHE534 Course Pack*. 2009.
4. Energy Minerals Division. Oil Sands.  
[http://emd.aapg.org/technical\\_areas/oil\\_sands.cfm](http://emd.aapg.org/technical_areas/oil_sands.cfm)
5. <http://www.womp-int.com/story/2009vol04/story027.htm>

6. Sanders, R. S.; Ferre, A. L.; Maciejewski, W. B.; Gillies, R. G.; Shook, C. A. Bitumen effects on pipeline hydraulics during oil sand hydrotransport. *The Canadian Journal of Chemical Engineering* **2000**, 78 (4), 731-742.
7. Liu, J.; Xu, Z.; Masliyah, J. Interaction between bitumen and fines in oil sands extraction system: Implication to bitumen recovery. *Canadian Journal of Chemical Engineering* **2004**, 82 (4), 655-666.
8. Wang, X. Polymer Aids for Settling and Filtration of Oil Sands Tailings. MSc Thesis, University of Alberta, Edmonton, 2010.
9. Zhu, R.; Liu, Q.; Xu, Z.; Masliyah, J. H.; Khan, A. Role of dissolving carbon dioxide in densification of oil sands tailings. *Energy & Fuels* **2011**, 25 (5), 2049-2057.
10. *Tailings, A Lasting Oil Sands Legacy*; WWF-Canada Tailings Report Summary: 2010.
11. Simeritsch, T.; Obad, J.; Dyer, S. *Tailings Plan Review*; The Pembina Institute and Water Matter: December 2009.
12. *ERCB Directive 074: Tailings Performance Criteria and Requirements for Oil Sands Mining Schemes*. February 2009.
13. *Oil Sands Tailings Technology Review*; BGC Engineering Inc.: July 2010.
14. Sworska, A.; Laskowski, J. S.; Cymerman, G. Flocculation of the Syncrude fine tailings: Part I. Effect of pH, polymer dosage and  $Mg^{2+}$  and  $Ca^{2+}$  cations. *International Journal of Mineral Processing* **2000**, 60 (2), 143-152.

15. Cymerman, G.; Kwong, T.; Lord, E.; Hamza, H.; Xu, Y. In *Proceedings of the 3rd UBC-McGill Biannual International Symposium on Fundamentals of Mineral Processing*, 1999; 1999; pp 605-619.
16. Masliyah, J. Processing of tailings in Canadian oil sands industry. *Trans. Nonferrous Met. Soc. China* **2002**, *12* (3), 524-528.
17. Li, H.; Long, J.; Xu, Z.; Masliyah, J. H. Flocculation of kaolinite clay suspensions using a temperature-sensitive polymer. *AIChE Journal* **2007**, *53* (2), 479-488.
18. Scott, J. D.; Ozum, B. *Oil Sans Tailings: What Needs to be Done*; MINING.com 2010, 14-16.
19. Purdy, B. G.; Macdonald, S. E.; Lieffers, V. Naturally Saline Boreal Communities as Models for Reclamation of Saline Oil Sands Tailings. *Restoration Ecology* **2005**, *13* (4), 667-677.
20. Tripathy, T.; De, B. R. Flocculation: A New Way to Treat the Waste Water. *Journal of Physical Sciences* **2006**, *10*, 93-127.
21. Owen, A. T.; Fawell, P. D.; Swift, J. D.; Farrow, J. B. The impact of polyacrylamide flocculant solution age on flocculation performance. *International Journal of Mineral Processing* **2002**, *67*, 123-144.
22. Ahmed, Z.; Mark, J. E. Biominetic materials: recent development in organic-inorganic hybrids. *Materials Science and Engineering C* **1998**, *6*, 183-196.
23. Chujo, Y. Organic-inorganic hybrid materials. *Solid State & Materials Science* **1996**, *1*, 806-811.

24. Novak, B. M. Hybrid nanocomposite materials-between inorganic glasses and organic polymers. *Advanced Materials* **1993**, 5 (6), 422-433.
25. Seddon, A. B. Sol-gel derived organic-inorganic hybrid materials for photobic applications. *IEE Proceedings: Circuits, Devices and Systems* **1998**, 145 (5), 369-372.
26. Yano, S.; Iwata, K.; Kurita, K. Physical properties and structure of organic-inorganic hybrid materials produced by sol-gel process. *Materials Science and Engineering C* **1998**, 6, 75-90.
27. Ye, H.; Zhao, J. Q.; Zhang, Y. H. Novel degradable superabsorbent materials of silicate/acrylic-base polymer hybrids. *Journal of Applied Polymer Science* **2004**, 91, 936-940.
28. Yang, W. Y.; Qian, J. W.; Shen, Z. Q. A novel flocculant of Al(OH)<sub>3</sub>-polyacrylamide ionic hybrid. *Journal of Colloid and Interface Science* **2004**, 273 (2), 400-405.
29. Sun, W.; Long, J.; Xu, Z.; Masliyah, J. H. Study of Al(OH)<sub>3</sub>-polyacrylamide-induced pelleting flocculation by single molecule force spectroscopy. *Langmuir* **2008**, 24 (24), 14015-14021.
30. Guo, L. Understanding Al-PAM Assisted Oil Sands Tailings Treatment. Oil Sands Research Group Student Presentation, University of Alberta, Edmonton, 2010.
31. Alagha, L.; Wang, S.; Xu, Z.; Masliyah, J. Adsorption Kinetics of a Novel Organic-Inorganic Hybrid Polymer on Silica and Alumina Studied by

Quartz Crystal Microbalance. *The Journal of Physical Chemistry C* **2011**, *115* (31), 15390-15402.

32. Wang, H.-L.; Cui, J.-Y.; Jiang, W.-F. Synthesis, characterization and flocculation activity of novel Fe(OH)<sub>3</sub>-polyacrylamide hybrid polymer. *Materials Chemistry and Physics* **2011**, *130* (3), 993-999.
33. Hu, Y. A Novel Fe-PAM Flocculant for Oil Sands Tailings Treatment. Oil Sands Research Group Student Presentation, Syncrude Research Centre, Edmonton, 2011.

## Chapter 3 Materials and Methodology

### 3.1 Materials

#### 3.1.1 Polymers

Three polymers were used in flocculation and adsorption tests: MF 1011, Al-PAM and Fe-PAM. MF 1011 was purchased from Ciba Chemicals (U.K.) and used without further purification. Al-PAM and Fe-PAM were in-house synthesized. Polymer stock solutions were prepared at a concentration of 1000 ppm one day prior to their use. Table 3-1 shows the different characteristics of the three polymers used in this study.

Table 3-1 Characteristics of Polymers Used in This Work

Polymer	Intrinsic Viscosity [ $\eta$ ] (mL/g)	MW ( $10^6$ Da)	Metal Content (wt%)	Type
Al-PAM	587	1.6	0.17	Cationic
Fe-PAM	583.5	1.6	0.16	Cationic
MF 1011	13968	17.5	0	Anionic

#### 3.1.2 Other Chemicals

Acid washed kaolin clay used to prepare model tailings was purchased from Fisher Scientific. Vacuum-distillation-feed bitumen used to prepare bitumen surfaces for adsorption tests and bitumen emulsions for zeta potential measurements was provided by Syncrude Canada Ltd. Silica- and alumina-coated

quartz crystal sensors used in polymer adsorption tests were purchased from Q-sense. Reagent grade hydrochloric acid and sodium hydroxide, used as pH modifiers, were purchased from Fisher Scientific. ACS certified toluene used as solvent for bitumen was also purchased from Fisher Scientific.

### 3.1.3 Preparation of Model Tailings

Model tailings were prepared with 5 wt% of kaolin suspended in plant recycle process water. The process water was supplied by Syncrude Canada Ltd. and its major ion concentration is shown in Table 3-2. The kaolin suspension was stirred with a magnetic stir bar overnight prior to settling or flocculation tests. The cumulative particle size distribution of model tailings was measured by a focused beam reflectance measurement (FBRM; Mettler Toledo, US). The FBRM probe was able to measure the chord length of the particles ranging from 1 to 1000  $\mu\text{m}$ . As shown in Figure 3-1,  $d_{50}$  of model tailings was 20.9  $\mu\text{m}$ . The pH values of model tailings were adjusted to 8.5 prior to settling or flocculation experiments.

Table 3-2 Average Concentration of Major Ion in Syncrude Process Water

Composition	Ca <sup>2+</sup>	Mg <sup>2+</sup>	K <sup>+</sup>	Na <sup>+</sup>	Cl <sup>-</sup>	NO <sup>3-</sup>	SO <sub>4</sub> <sup>2-</sup>	HCO <sub>3</sub> <sup>-</sup>
ppm	33.5	16.9	23.8	508.4	389.5	3.4	87.1	741.2

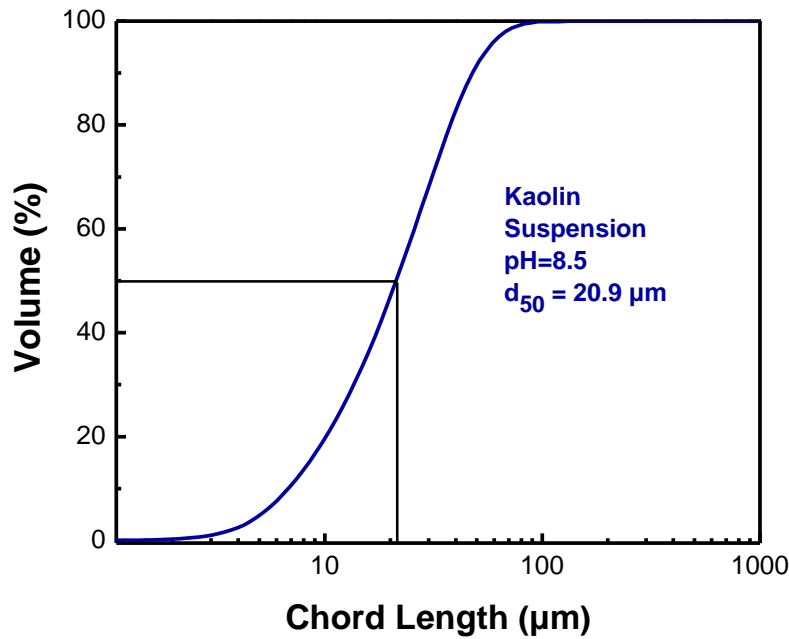


Figure 3-1 Cumulative Particle Size Distribution of Model Tailings

### 3.1.4 Preparation of Laboratory Extraction Tailings

Laboratory extraction tailings were obtained from an oil sand ore provided by Canadian Natural Resources Ltd. The ore contains 8.3% bitumen, 7.4% water and 84.3% solids by weight. The bitumen extraction tests were conducted in a Denver Flotation Cell at 35 °C. About 950 mL Syncrude process water was adjusted to pH 8.5 and mixed with 300 g oil sand ore. After 5 minutes of conditioning the slurry at 1000 rpm, air was introduced at 150 mL/min and bitumen froth was skimmed for 20 minutes. Tailings slurry left in the Denver Cell was collected into a 4 L glass jar. To prevent settling of tailings, the slurry was stirred at 600 rpm for 4 hours by a four-bladed stainless steel impeller (2 inch diameter) with an IKA Digital Stirrer before settling and flocculation tests. The composition of tailings

was determined by Dean-Stark apparatus with toluene as the reflux solvent [1]. Fines are defined as mineral solids with particle size less than 44  $\mu\text{m}$  and their content in solids was determined by wet-screen using a 44  $\mu\text{m}$  sieve. The weight percentages of water, bitumen, solids and fines in solids in laboratory extraction tailings are listed in Table 3-3. The cumulative particle size distribution of laboratory extraction tailings is shown in Figure 3-2. The  $d_{50}$  of laboratory extraction tailings was 29.6  $\mu\text{m}$  and the pH of tailings slurry was  $\sim 8.5$ .

Table 3-3 Average Composition of Laboratory Extraction Tailings

Component	Water	Bitumen	Solids	Fines in Solids
wt%	83.1	1.6	15.3	51

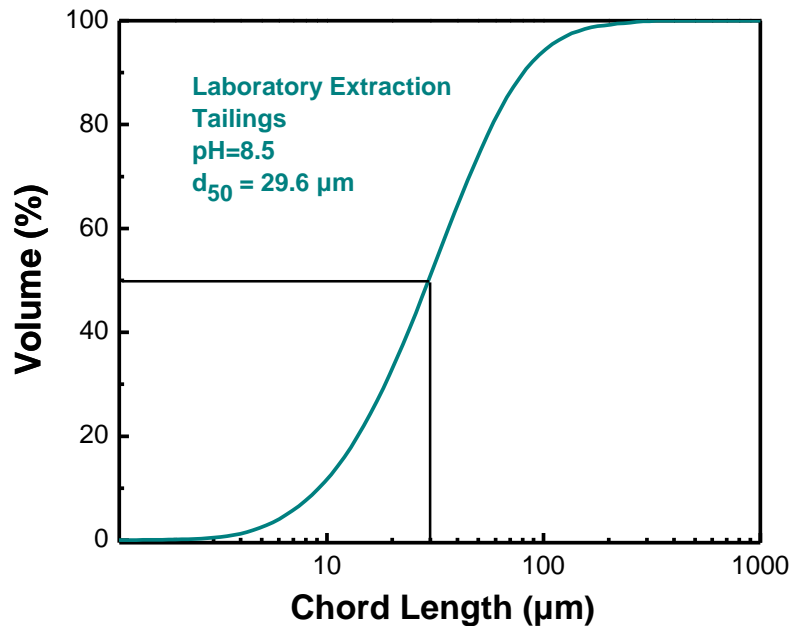


Figure 3-2 Cumulative Particle Size Distribution of Laboratory Extraction Tailings

### **3.2 Settling Test of Model and Laboratory Extraction Tailings**

Settling tests for both model and laboratory extraction tailings were performed in process water. In a typical settling experiment, 95 g of model or laboratory extraction tailings were placed in a 250 mL beaker. The slurry was first stirred at 500 rpm for 2 minutes using an IKA RW20 digital stirrer. The stirring rate was then reduced to 350 rpm before the desired polymer solution was added at a specific dosage. The polymer dosage (ppm) was expressed based on the final volume of the suspension. After the completion of polymer addition, the agitation was stopped immediately or after pre-determined extended mixing time. The flocculated slurry was transferred to a 100 mL graduated cylinder and the suspension mudline height was measured as a function of settling time ( $t$ ). The settling curves were obtained by plotting the normalized mudline height ( $h/H$ , where “ $h$ ” is the mudline height at settling time “ $t$ ” and “ $H$ ” is the initial mudline height) versus settling time. The initial slope of the settling curve was taken as initial settling rate (ISR), and used as a measure of flocculation performance of different polymers [2].

### **3.3 Flocculation Test Monitored by FBRM**

The flocculation dynamics and floc properties of model and laboratory extraction tailings were investigated using FBRM. Prior to each measurement, the FBRM probe window was thoroughly cleaned and the accuracy of the probe is tested with deionized water. A total background count of less than 150 counts per second is required in this study. After the background count was determined to be less than 150 counts per second, the FBRM probe was immersed in 100 mL of

model or laboratory extraction tailings. Slurries were stirred at 400 rpm and 650 rpm for model and laboratory extraction tailings, respectively, to prevent settling of solids. After a steady FBRM reading was obtained, polymer solutions were added at different dosages and the stirring rate was kept constant during the experiment. The flocculation process was monitored for 1 hour for each polymer at a specific dosage in order to study the stability of flocs formed with different polymer flocculants.

### **3.4 Zeta Potential Measurement**

#### **3.4.1 Model Tailings (Kaolin Suspensions)**

Zeta potential of model tailings was measured using Zeta PALS (Brookhaven Instruments Corp., New York). Measurements were undertaken before and after the addition of polymers at various dosages in order to understand the mechanism of interactions between kaolin particles and different polymers used in this study, including cationic hybrids (Fe-PAM and Al-PAM) and anionic MF 1011. Kaolin suspensions used in zeta potential measurement were prepared with 0.01 wt% of kaolin in process water. The process water was filtered using Milli-pore filters (Millipore) with 0.1  $\mu\text{m}$  pore size to remove any fine solids [3]. Kaolin suspensions were then placed in the shaker for overnight and the pH was adjusted to 8.5 before experiments. A Polymer solution was then added at a specific dosage and the sample was conditioned in an ultrasonic bath (Fisher Scientific) for 15 minutes before zeta potential measurements were conducted. The average values of five individual measurements were reported in this study.

### **3.4.2 Laboratory Extraction Tailings**

To investigate the effect of polymer addition on the flocculation of laboratory extraction tailings, zeta potentials of bitumen and fines were measured using a Zetaphoremeter Z3110 (CAD Instrumentation, France). Emulsified bitumen suspension was prepared by dispersing 1 g of vacuum-distillation feed bitumen in 100 mL filtered process water using an ultrasonic dismembrator. Bitumen suspensions were allowed to “cream” for 30 minutes and a sample of each suspension was diluted to 0.01-0.05 wt%. Fine solids obtained from laboratory extraction tailings were used to prepare 0.01-0.05 wt% of fine particle slurries in process water by the ultrasonic dismembrator [4]. For each measurement, the desired polymer solution was added at a predetermined dosage, and the sample was conditioned in an ultrasonic bath for another 15 minutes to ensure sufficient interactions between polymer and particles or bitumen droplets. All measurements were carried out at room temperature and pH 8.5. The average of ten independent experiments was reported.

### **3.5 Measurement of Total Organic Carbon (TOC)**

Total dissolved organic carbon measurements were conducted to determine the amount of polymer adsorbed on model tailings during the flocculation process. Total Organic Carbon Analyzer (SHIMADZU, Japan) was used to measure the TOC concentration in supernatants after flocculation. To remove any solids that may block the instrument, the supernatant was collected to a centrifuge tube and centrifuged at 15000 rpm for 30 minutes [5]. The supernatant in the centrifuge

tube was used in TOC measurements. Blank tests were conducted after centrifuging polymer solutions prepared in deionized water to ensure that the centrifugation does not alter the amount of polymers present in the original samples.

In each test, the sample was delivered to a combustion furnace heated to 680 °C, where it was burnt completely and converted to carbon dioxide. The carbon dioxide was then cooled, dehumidified and detected by an infrared gas analyzer. The total carbon (TC) concentration in the sample was obtained through comparison with a calibration curve. Furthermore, the oxidized sample underwent a sparging process, where the inorganic carbon (IC) was converted to carbon dioxide, and the IC concentration was detected by the infrared gas analyzer. The TOC concentration in the sample was calculated by subtracting the IC concentration from TC concentration [6].

### **3.6 Adsorption Test Monitored by QCM-D**

#### **3.6.1 Preparation of Bitumen Surfaces for QCM-D Experiment**

Silicon dioxide coated sensors purchased from Q-Sense were used as substrates for preparation of bitumen-coated surfaces for polymer adsorption tests on bitumen. Prior to bitumen coating, sensors were cleaned with 2 wt% SDS solutions, rinsed with deionized water, dried with nitrogen and placed in an UV-ozone for 20 minutes [7]. To ensure the stability of coated bitumen layer, the cleaned silica sensors were first silylated by exposing to the vapor of dichlorodimethylsilane  $[(\text{CH}_3)_2\text{SiCl}_2]$  for 60 seconds. Sensors were then baked

under vacuum at 80 °C for overnight. The thickness of a silane layer coated on a silica sensor was measured by Q-Sense 401 software and determined to be ~ 5 nm. After silylation, hydrophobic silica surfaces were coated with bitumen using a P670 spin-coater (Specialty Coating Systems Inc.) operated as follows: five drops of 10 wt% bitumen in toluene solution were added slowly to the center of the silylated sensor spinning at 2000 rpm within 20 seconds, and then the spinning rate was increased to 4000 rpm for 1 minute to obtain a smooth, dry and uniform bitumen layer [8]. The typical thickness of bitumen layer coated on silylated silica surface was determined to be ~ 350 nm.

### **3.6.2 QCM-D Experiment**

The adsorption kinetics of polymer solutions on silica-, alumina- and bitumen-coated surfaces in filtered process water was determined using a QCM-D from Q-sense (Gothenburg, Sweden). For adsorption tests conducted on silica and alumina, sensors were washed with ethanol and 2% Hellmanex (HellmaGmbH) prior to each experiment, followed by thorough rinsing with deionized water and blow-drying with nitrogen. Sensors were then placed in an UV-ozone for 20 minutes to remove any organic contamination.

In each QCM-D experiment, deionized water was first pumped through the flow module by an IPC-N peristaltic pump (Ismatec, Switzerland) at 0.15 mL/min to establish a stable baseline [9]. To simulate the adsorption of polymers on solid surfaces during the flocculation process, filtered process water was then pumped into the chamber until the adsorption of ions in process water on the sensor reached equilibrium plateau. Polymer solution, prepared by adding polymer stock

solution at a specific dosage to filtered process water, was then introduced into the flow module at the same flow rate until a new equilibrium was achieved. The final step of each experiment was to wash the adsorbed polymer film with filtered process water again to check whether the adsorption is reversible or not. All the experiments were conducted at room temperature and pH 8.5. The third, fifth and seventh overtones were used in the Voigt model to estimate the adsorbed mass due to their stable responses.

## References

1. Bulmer, J. T.; Starr, J. *Syncrude Analytical Methods for Oil Sand and Bitumen Processing*; Alberta Oil Sands Technology and Research Authority (AOSTRA): Edmonton, Alberta, Canada, 1979.
2. Zhu, R.; Liu, Q.; Xu, Z.; Masliyah, J. H.; Khan, A. Role of dissolving carbon dioxide in densification of oil sands tailings. *Energy & Fuels* **2011**, 25 (5), 2049-2057.
3. Wu, C. A Fundamental Study of Bubble-Particle Interactions through Zeta-Potential Distribution Analysis. MSc Thesis, University of Alberta, Edmonton, 2011.
4. Liu, J.; Zhou, Z.; Xu, Z.; Masliyah, J. Bitumen-clay interactions in aqueous media studied by zeta potential distribution measurement. *Journal of Colloid and Interface Science* **2002**, 252 (2), 409-418.
5. Liu, J.; Xu, Z.; Masliyah, J. Interaction between bitumen and fines in oil sands extraction system: Implication to bitumen recovery. *The Canadian Journal of Chemical Engineering* **2004**, 82 (4), 655-666.

6. <http://www.shimadzu.com/an/toc/lab/toc-1.html>
7. Wang, S.; Segin, N.; Wang, K.; Masliyah, J. H.; Xu, Z. Wettability control mechanism of highly contaminated hydrophilic silica/alumina surfaces by ethyl cellulose. *The Journal of Physical Chemistry C* **2011**, *115* (21), 10576-10587.
8. Liu, J.; Xu, Z.; Masliyah, J. Studies on bitumen-silica interaction in aqueous solutions by atomic force microscopy. *Langmuir* **2003**, *19* (9), 3911-3920.
9. Alagha, L.; Wang, S.; Xu, Z.; Masliyah, J. Adsorption Kinetics of a Novel Organic–Inorganic Hybrid Polymer on Silica and Alumina Studied by Quartz Crystal Microbalance. *The Journal of Physical Chemistry C* **2011**, *115* (31), 15390-15402.

## **Chapter 4 Synthesis and Characterization of Inorganic-organic Hybrid Polymers**

Al-PAM and Fe-PAM were synthesized by polymerization of acrylamide monomers in  $\text{Al}(\text{OH})_3$  or  $\text{Fe}(\text{OH})_3$  colloidal suspensions. The obtained polymer gels were then purified by acetone and dried in a vacuum oven.

### **4.1 Materials**

Aluminum chloride, ferric chloride, ammonium carbonate, acrylamide monomers, ammonium persulfate and sodium bisulfite were used in the synthesis of Al-PAM and Fe-PAM. Acetone was used to purify Al-PAM and Fe-PAM gels. Hydrochloric acid and sodium hydroxide were used as pH modifiers. All chemicals were reagent grade and purchased from Fisher Scientific.

### **4.2 Synthesis of Inorganic-organic Hybrid Polymers**

#### **4.2.1 Synthesis of Al-PAM**

To synthesize Al-PAM, the first step is the preparation of  $\text{Al}(\text{OH})_3$  colloids. In this step, 29 mL of 1.54 M  $(\text{NH}_4)_2\text{CO}_3$  solution was added to 60 mL of 0.6 M  $\text{AlCl}_3$  solution by a Master FLEX C/L mini pump at a flow rate of 0.13 g/min. The  $\text{AlCl}_3$  solution was kept under stirring by an IKA RW20 digital stirrer at 500 rpm. When the addition of  $(\text{NH}_4)_2\text{CO}_3$  solution was completed, the mixture was stirred at 300 rpm for 1 hour to complete the reaction. The ideal  $\text{Al}(\text{OH})_3$  colloids for Al-PAM synthesis would have a particle size of 50-65 nm and zeta potential of 27-30 mV [1].

The second step is the polymerization of acrylamide monomers in an  $\text{Al}(\text{OH})_3$  colloidal suspension with  $(\text{NH}_4)_2\text{S}_2\text{O}_8/\text{NaHSO}_3$  as initiator. In this case, 4.5 g of acrylamide was added to 25.5 g of  $\text{Al}(\text{OH})_3$  colloidal suspension in a 250 mL 3-neck round bottom flask. The mixture was stirred with an IKA RW20 digital stirrer at 200 rpm, and nitrogen gas was purged to the system for 30 minutes to remove the oxygen which may exist. Then 2 mL of 500 ppm  $(\text{NH}_4)_2\text{S}_2\text{O}_8$  and 1000 ppm  $\text{NaHSO}_3$  solutions at 1:1 ratio was added slowly to the mixture to initiate the polymerization of acrylamide in  $\text{Al}(\text{OH})_3$  colloidal suspension. The reaction was kept running overnight at 40 °C [1].

#### **4.2.2 Synthesis of Fe-PAM**

Similar to that of Al-PAM, the first step in the synthesis of Fe-PAM is the preparation of  $\text{Fe}(\text{OH})_3$  colloidal suspension. In this step, 0.1 M  $(\text{NH}_4)_2\text{CO}_3$  solution was added to 25 g of 0.1 M  $\text{FeCl}_3$  solution at 0.5 g/min rate using a Master FLEX C/L mini pump. The  $\text{FeCl}_3$  solution was kept under stirring by an IKA RW20 digital stirrer at 500 rpm. The addition of  $(\text{NH}_4)_2\text{CO}_3$  solution was stopped when the pH of the mixture reached ~3.6. The mixture was then gently stirred at 300 rpm for 30 min to complete the reaction. The suitable  $\text{Fe}(\text{OH})_3$  colloids for Fe-PAM synthesis would have a particle size of 25-30 nm and zeta potential of 25-30 mV [2].

The second step is the polymerization of acrylamide monomers in a  $\text{Fe}(\text{OH})_3$  colloidal suspension with  $(\text{NH}_4)_2\text{S}_2\text{O}_8/\text{NaHSO}_3$  as initiator. In this step, 4.5 g of acrylamide was added to 25.5 g of fresh  $\text{Fe}(\text{OH})_3$  colloidal suspension in a 250 mL 3-neck round bottom flask. The mixture was stirred with an IKA RW20

digital stirrer at 200 rpm, and nitrogen gas was purged to the system for 30 minutes to remove oxygen which may exist. Then 2 mL initiator mixture (500 ppm  $(\text{NH}_4)_2\text{S}_2\text{O}_8$  and 1000 ppm  $\text{NaHSO}_3$  at 1:1 ratio) was added slowly to the flask to initiate the polymerization of acrylamide in  $\text{Fe}(\text{OH})_3$  colloidal suspension. The reaction was kept running overnight at 40 °C [2]. It should be noted that this synthesis procedure is different from what was reported in literature [3].

#### **4.2.3 Purification of Al-PAM and Fe-PAM**

The obtained Al-PAM or Fe-PAM polymer gel was diluted by Milli-Q water to 10 wt% and placed in a shaker for 2-3 days. Then the polymer solution was added dropwise into acetone (the volume ratio of acetone to polymer solution is ~ 5) to remove un-reacted  $\text{Al}(\text{OH})_3$  or  $\text{Fe}(\text{OH})_3$  colloid and acrylamide. The purified polymer gel in the form of precipitates in acetone was collected to a Teflon dish and dried in a vacuum oven at 40 °C overnight [2, 4].

### **4.3 Characterization of Al-PAM and Fe-PAM**

#### **4.3.1 Molecular Weight**

The molecular weight of the synthesized Al-PAM and Fe-PAM was calculated from the Mark-Houwink equation:

$$[\eta] = KM_v^a$$

where  $K$  and  $a$  are characteristic constants for a given polymer-solvent system at a specific temperature.  $M_v$  is the viscosity-average molecular weight and  $[\eta]$  is the intrinsic viscosity.

The intrinsic viscosity of Al-PAM or Fe-PAM was measured using an Ubbelohde viscometer (Fisher Scientific) at 25 °C. The flux time was recorded with an accuracy of  $\pm 0.05$  s. According to the Huggins equation:

$$[\eta] = \lim_{c \rightarrow 0} [(\eta - \eta_0)/\eta_0 c] = \lim_{c \rightarrow 0} (\eta_{sp}/c)$$

where  $\eta$  is the viscosity of a polymer solution at concentration  $c$ ,  $\eta_0$  is the viscosity of pure solvent,  $\eta_{sp}$  is the specific viscosity,  $c$  is the concentration of polymer solution in g/L, and  $[\eta]$  is the intrinsic viscosity. At each concentration, both reduced viscosity,  $\eta_{sp}/c$  and inherent viscosity  $\ln(\eta/\eta_0)/c$  were determined and plotted as a function of the polymer concentration. By extrapolation of both data sets, the y-intercepts should fall on the same point, which is known as the intrinsic viscosity of the polymer [1, 5, 6].

#### **4.3.2 Metal Content**

The metal content of Al-PAM or Fe-PAM was measured by atomic absorption spectroscopy (AAS). This technique relies on the Beer-Lambert law to determine the concentration of a specific element in a sample. The electrons of the atoms can be promoted to higher energy orbitals by absorbing light at a particular wavelength. Each wavelength corresponds to only one element. During an atomic absorption test, a known amount of energy is passed through the atomized sample, and by measuring the quantity of light remained after absorption, the concentration of the element can be determined [7]. The samples used in our measurements were 10 mL 1000 ppm Al-PAM and Fe-PAM. The characteristics of Al-PAM and Fe-PAM were shown in Table 4-1.

Table 4-1 Characteristics of Al-PAM and Fe-PAM

Polymer	Colloid Properties		$[\eta]$ (mL/g)	MW ( $10^6$ Da)	Metal Content (wt %)
	Particle Size (nm)	Zeta Potential (mV)			
Al-PAM	35.0	29.8	587	1.6	0.17
Fe-PAM	25.2	26.8	583.5	1.6	0.16

### References

1. Alagha, L.; Wang, S.; Xu, Z.; Masliyah, J. Adsorption Kinetics of a Novel Organic–Inorganic Hybrid Polymer on Silica and Alumina Studied by Quartz Crystal Microbalance. *The Journal of Physical Chemistry C* **2011**, *115* (31), 15390-15402.
2. Hu, Y. A Novel Fe-PAM Flocculant for Oil Sands Tailings Treatment. Oil Sands Research Group Student Presentation, Syncrude Research Centre, Edmonton, 2011.
3. Wang, H.-L.; Cui, J.-Y.; Jiang, W.-F. Synthesis, characterization and flocculation activity of novel Fe(OH)<sub>3</sub>-polyacrylamide hybrid polymer. *Materials Chemistry and Physics* **2011**, *130* (3), 993-999.
4. Yang, W. Y.; Qian, J. W.; Shen, Z. Q. A novel flocculant of Al(OH)<sub>3</sub>-polyacrylamide ionic hybrid. *Journal of Colloid and Interface Science* **2004**, *273* (2), 400-405.

5. Li, H.; Long, J.; Xu, Z.; Masliyah, J. H. Flocculation of kaolinite clay suspensions using a temperature-sensitive polymer. *AICHE Journal* **2007**, *53* (2), 479-488.
6. Barbara, H., *Polymer Analysis*. New York: Wiley: 2002.
7. [http://en.wikipedia.org/wiki/Atomic\\_absorption\\_spectroscopy](http://en.wikipedia.org/wiki/Atomic_absorption_spectroscopy)

## **Chapter 5 Flocculation of Model Tailings**

Al-PAM, Fe-PAM and MF 1011 were used to flocculate model tailings. The model tailings were prepared with 5 wt% of kaolin in process water. As shown in Figure 3-1,  $d_{50}$  of model tailings was 20.9  $\mu\text{m}$ . The pH of model tailings was adjusted to 8.5 before experiment.

### **5.1 Effect of Al-PAM on Flocculation**

For a typical test, after adding polymer to tailings slurry, the  $d_{50}$  of particles will increase, reach maximum and then decrease. This type of patterns indicates the formation and breakage of flocs. For example, the particle size evolution of model tailings after addition of Al-PAM is shown in Figure 5-1. It is clearly demonstrated that upon the addition of 10 ppm Al-PAM, the  $d_{50}$  of the model tailings increased significantly, reached the maximum at 100 seconds and then decreased. In all our tests, the flocculation time that the flocs evolved to the maximum  $d_{50}$  was between 90 seconds and 110 seconds. For the simplicity of data presentation, the maximum  $d_{50}$  of tailings after polymer addition was reported and compared in this work.

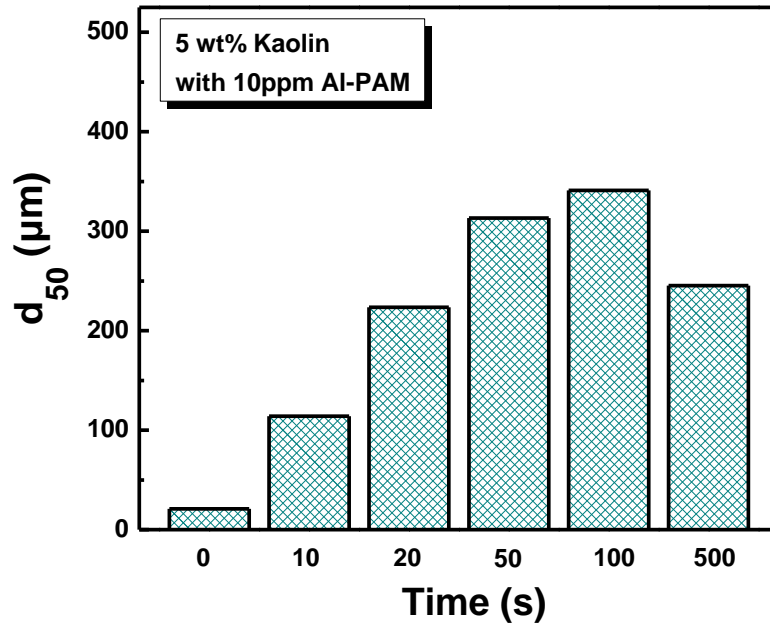


Figure 5-1 Particle Size Evolution of Model Tailings after the Addition of 10 ppm Al-PAM

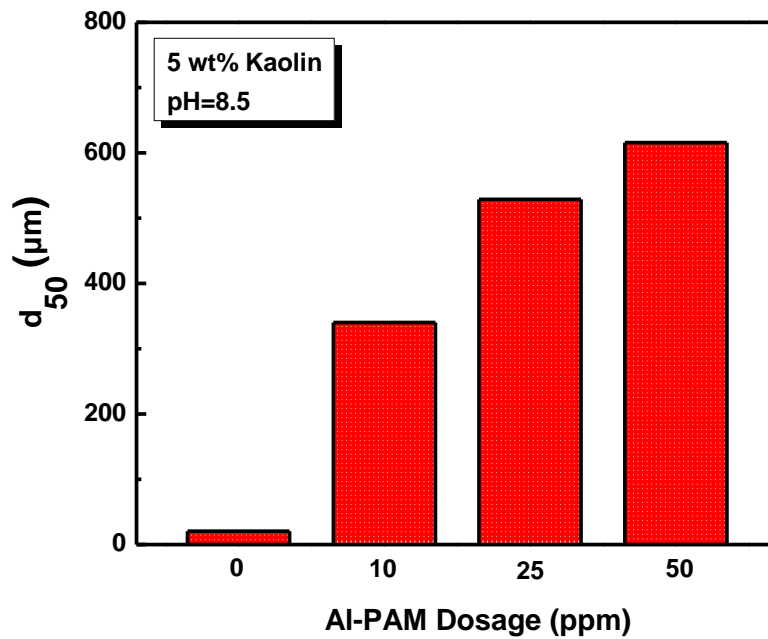


Figure 5-2 Effect of Al-PAM Dosage on Maximum  $d_{50}$  of Model Tailings

Figure 5-2 shows the effect of Al-PAM addition on maximum  $d_{50}$  of model tailings. The maximum  $d_{50}$  of model tailings increased from 20.9  $\mu\text{m}$  to 340  $\mu\text{m}$ , 529  $\mu\text{m}$  and 616  $\mu\text{m}$  upon the addition of 10 ppm, 25 ppm and 50 ppm Al-PAM, respectively. Increment in Al-PAM dosage led to an increase in maximum  $d_{50}$  of model tailings, which could be attributed to an increase in surface coverage of particles in model tailings by Al-PAM. It suggests that Al-PAM at higher dosage induces the formation of larger flocs. Above 50 ppm, further increment in polymer dosage led to the formation of some flocs with chord length larger than 1000  $\mu\text{m}$ , which exceeded the measurement range of FBRM probe. For this reason, the tests were stopped at 50 ppm polymer addition.

## 5.2 Effect of Fe-PAM on Flocculation

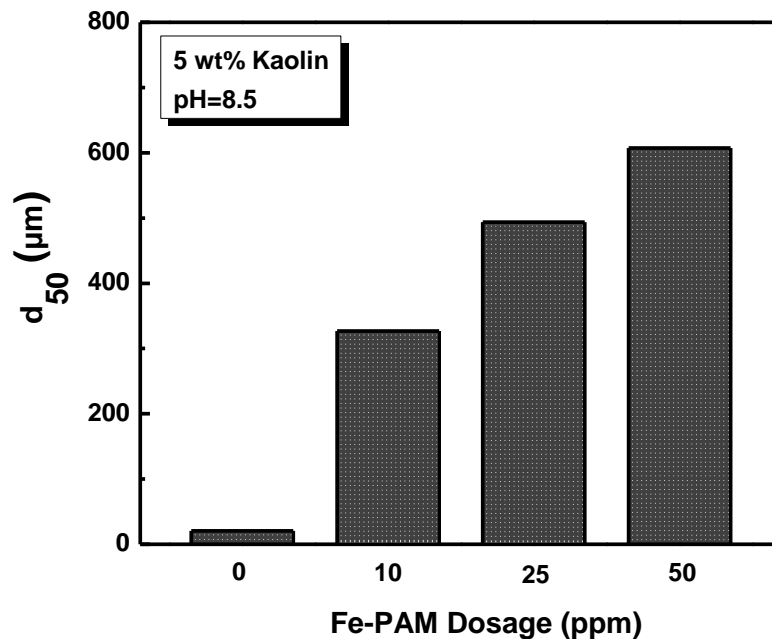


Figure 5-3 Effect of Fe-PAM Dosage on Maximum  $d_{50}$  of Model Tailings

Figure 5-3 shows the effect of Fe-PAM on maximum  $d_{50}$  of model tailings. Similar to that of Al-PAM, remarkable increase in maximum  $d_{50}$  of model tailings was observed upon Fe-PAM addition. At 10 ppm, 25 ppm and 50 ppm, Fe-PAM increased the maximum  $d_{50}$  of model tailings from 20.9  $\mu\text{m}$  to 327  $\mu\text{m}$ , 494  $\mu\text{m}$  and 608, respectively. Higher dosage of Fe-PAM led to more efficient aggregation of model tailings.

### 5.3 Effect of MF 1011 on Flocculation

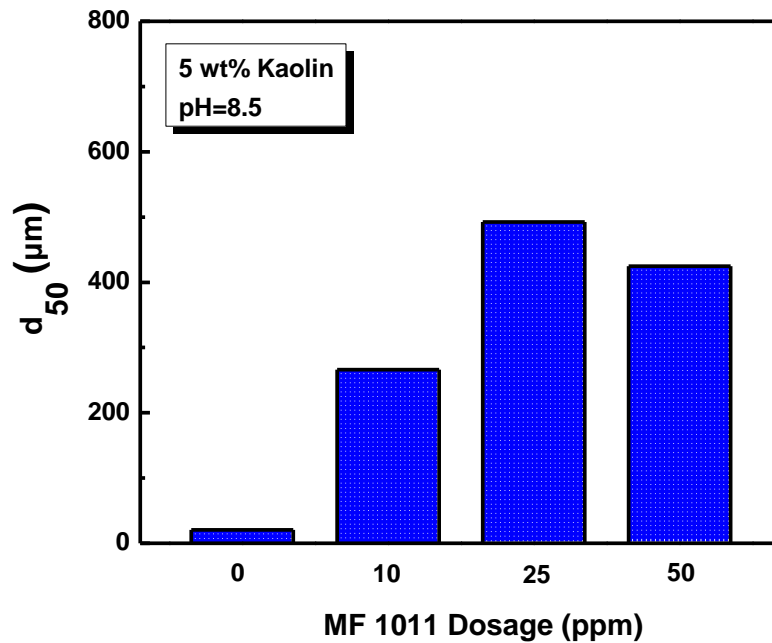


Figure 5-4 Effect of MF 1011 Dosage on Maximum  $d_{50}$  of Model Tailings

As shown in Figure 5-4, upon addition of 10 ppm, 25 ppm and 50 ppm MF 1011, the maximum  $d_{50}$  of model tailings increased from 20.9  $\mu\text{m}$  to 266  $\mu\text{m}$ , 492  $\mu\text{m}$

and 425  $\mu\text{m}$ , respectively. MF 1011 exhibited an optimum dosage at 25 ppm. Further increment in dosage resulted in a decrease in maximum  $d_{50}$  of model tailings, which could be attributed to the steric stabilization of kaolin particles with excessive polymer on their surfaces [1].

#### 5.4 Comparison among Al-PAM, Fe-PAM and MF 1011

The flocculation performance of in-house synthesized Al-PAM, Fe-PAM and a commercial flocculant MF 1011 was compared at all tested dosages, in terms of the maximum  $d_{50}$  of flocs.

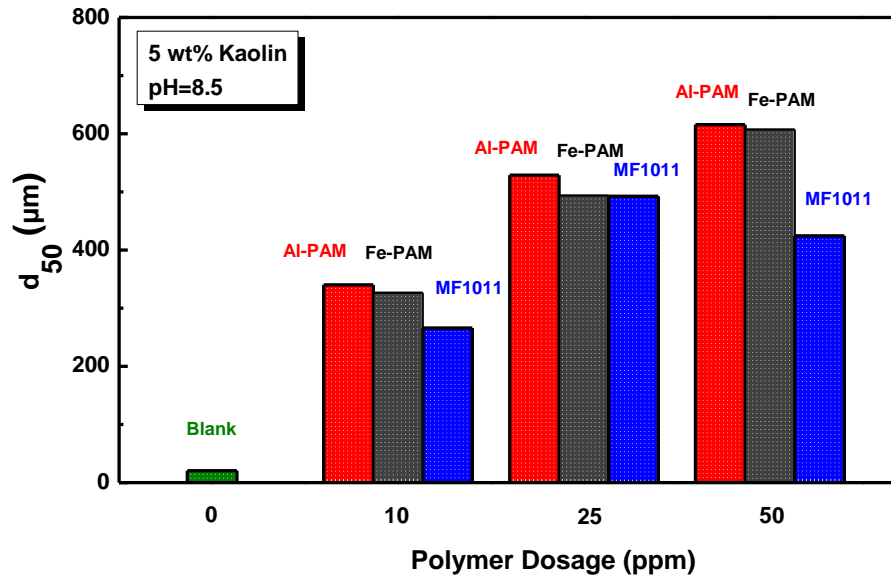


Figure 5-5 Comparison among Al-PAM, Fe-PAM and MF 1011

Figure 5-5 shows that adding polymer to model tailings dramatically increased the maximum  $d_{50}$  of kaolin particles. The effects of Al-PAM and Fe-PAM on  $d_{50}$  of model tailings are very similar at all tested dosages. At 10 ppm, 25 ppm and 50 ppm, both hybrid polymers increased the maximum  $d_{50}$  of model tailings from

20.9  $\mu\text{m}$  to  $\sim 330 \mu\text{m}$ , 500  $\mu\text{m}$  and 610  $\mu\text{m}$ , respectively. Increasing polymer dosage led to the formation of larger flocs. However, further increment in MF 1011 dosage resulted in a decreased maximum  $d_{50}$  of model tailings, due to the overdose effect. The enhanced floc size by cationic hybrid polymers, Al-PAM and Fe-PAM, could be attributed to the strong adsorption of both polymers on model tailings through both charge neutralization and hydrogen bonding mechanisms, which eventually led to the formation of larger and denser flocs, and better performance than anionic MF 1011 [2].

### **5.5 Strength of Flocs Formed by Different Polymers**

To study the stability of flocs formed by different flocculants under shear, the flocculation of model tailings by Al-PAM, Fe-PAM and MF 1011 was monitored by FBRM for 1 hour. The FBRM probe was immersed in 100 mL of model tailings. After stirring the slurry at 400 rpm for 5 minutes, Al-PAM, Fe-PAM and MF 1011 were added at 50 ppm, 50 ppm and 25 ppm dosages, respectively. The stirring rate was kept at 400 rpm during the experiment. Figure 5-6 shows the  $d_{50}$  of model tailings with polymers as a function of time. It is clearly demonstrated that, after adding flocculants, the  $d_{50}$  of model tailings significantly increased and reached maximum value. For 50 ppm Al-PAM, 50 ppm Fe-PAM and 25 ppm MF 1011, the maximum  $d_{50}$  was  $\sim 610 \mu\text{m}$ , 610  $\mu\text{m}$  and 500  $\mu\text{m}$ , respectively. During 1 hour stirring at 400 rpm, no significant change in the  $d_{50}$  of model tailings was observed. This observation indicates the formation of large and stable flocs upon addition of each polymer at its optimum dosage. Furthermore, flocs formed were resistant to the shearing forces at the stirring rate used in this experiment.

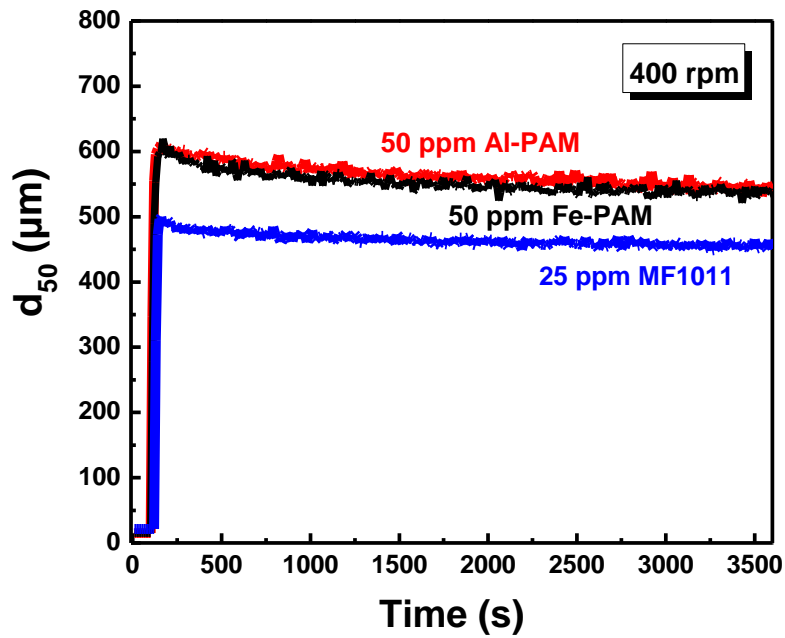


Figure 5-6  $d_{50}$  of Model Tailings with Polymer Addition as a Function of Time

### 5.6 Effect of Mixing Method on Flocculation

Mixing method is an important factor that can affect flocculation process. The flocculation of model tailings without and with baffle was studied. As shown in Figure 5-7, with baffle, the maximum  $d_{50}$  of model tailings with each polymer addition decreased by 100  $\mu\text{m}$ . This could be attributed to more sufficient mixing with baffle: some large flocs hit the baffle and were broken, thus decreasing the maximum  $d_{50}$  of the flocs.

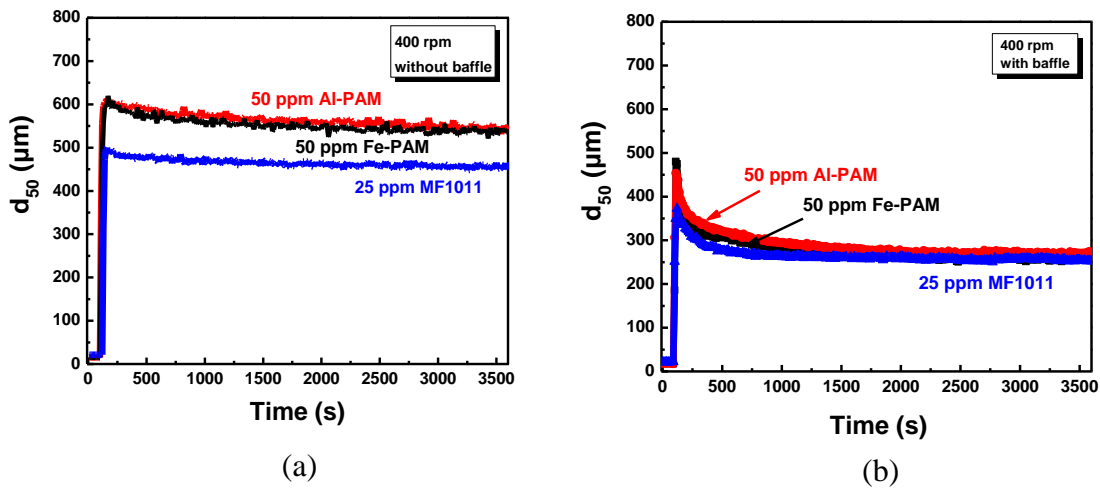


Figure 5-7 Effect of Mixing Method on Flocculation (a) Stirring at 400 rpm without Baffle; (b) Stirring at 400 rpm with Baffle

### 5.7 Effect of Stirring Rate on Flocculation

Higher stirring rate may generate larger shear force, which could create significant influence on the flocculation process. The effect of stirring rate on flocculation of model tailings was shown in Figure 5-8. It is clearly shown that compared with mixing at 400 rpm, mixing at 650 rpm dramatically decreased the maximum  $d_{50}$  of model tailings after polymer addition. For model tailings flocculated by Al-PAM or Fe-PAM, the maximum  $d_{50}$  decreased from  $\sim 610 \mu\text{m}$  to  $300 \mu\text{m}$ . For model tailings flocculated by MF 1011, the maximum  $d_{50}$  decreased from  $\sim 500 \mu\text{m}$  to  $350 \mu\text{m}$ . This observation indicates the breakage of large flocs at higher stirring rate [3].

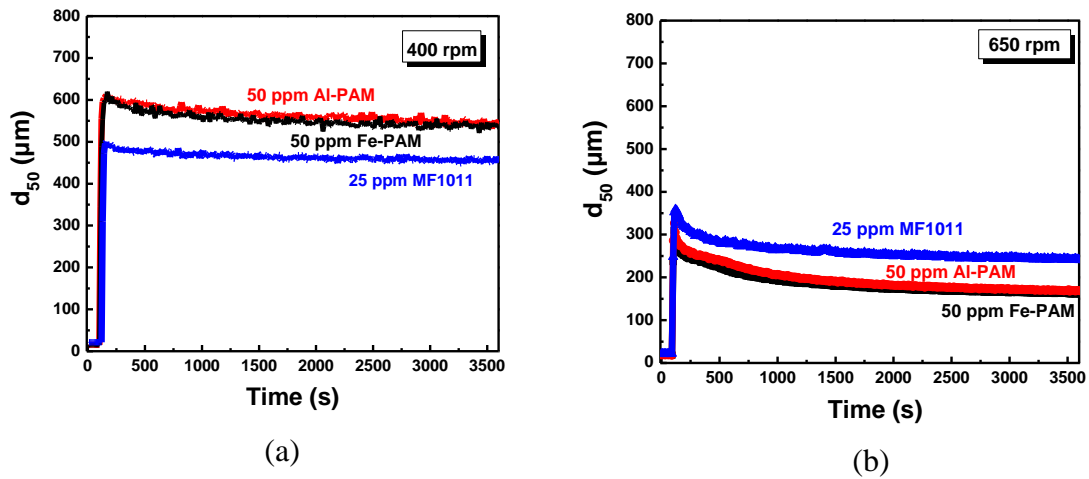


Figure 5-8 Effect of Stirring Rate on Flocculation (a) Stirring at 400 rpm; (b) Stirring at 650 rpm

## 5.8 Summary

Al-PAM, Fe-PAM and MF 1011 were found to be very effective in flocculation of model tailings (5 wt% kaolin suspensions). At 50 ppm, 50 ppm and 25 ppm dosage of Al-PAM, Fe-PAM and MF 1011, the maximum  $d_{50}$  of model tailings increased from 20.9  $\mu\text{m}$  to  $\sim 610 \mu\text{m}$ , 610  $\mu\text{m}$  and 500  $\mu\text{m}$ , respectively. Raising hybrid polymer dosage led to the formation of larger flocs due to an increased surface coverage of solids by polymers. In fact, the size of some flocs at Al-PAM or Fe-PAM dosage over 50 ppm exceeded the measurement range of FBRM. MF 1011 showed an optimum dosage of 25 ppm, further increment in its dosage resulted in a decrease in the maximum  $d_{50}$  of model tailings, which could be attributed to the steric stabilization of kaolin particles by excessive polymer on their surfaces. The maximum  $d_{50}$  of model tailings was significantly influenced by mixing method and stirring rate. With baffle, the maximum  $d_{50}$  of model tailings

with each polymer addition decreased by 100  $\mu\text{m}$ . When increasing the stirring rate from 400 rpm to 650 rpm, the maximum  $d_{50}$  of model tailings with either Al-PAM or Fe-PAM addition decreased from  $\sim 610$   $\mu\text{m}$  to 300  $\mu\text{m}$ . For model tailings flocculated by MF 1011, the maximum  $d_{50}$  decreased from  $\sim 500$   $\mu\text{m}$  to 350  $\mu\text{m}$ . This observation indicates that large flocs broke at higher stirring rate.

## References

1. Li, H.; Long, J.; Xu, Z.; Masliyah, J. H. Synergetic role of polymer flocculant in low-temperature bitumen extraction and tailings treatment. *Energy & Fuels* **2005**, *19* (3), 936-943.
2. Alagha, L.; Wang, S.; Xu, Z.; Masliyah, J. Adsorption Kinetics of a Novel Organic-Inorganic Hybrid Polymer on Silica and Alumina Studied by Quartz Crystal Microbalance. *The Journal of Physical Chemistry C* **2011**, *115* (31), 15390-15402.
3. Alfano, J. C.; Carter, P. W.; Dunham, A. J.; Nowak, M. J.; Tubergen, K. R. Polyelectrolyte-induced aggregation of microcrystalline cellulose: Reversibility and shear effects. *Journal of Colloid and Interface Science* **2000**, *223* (2), 244-254.

## Chapter 6 Adsorption of Polymers on Model Tailings

### 6.1 Interaction of Polymers with Model Tailings

The interactions of different polymers with model tailings were investigated by measuring zeta potentials of kaolin particles before and after polymer addition.

Results are shown in Figure 6-1.

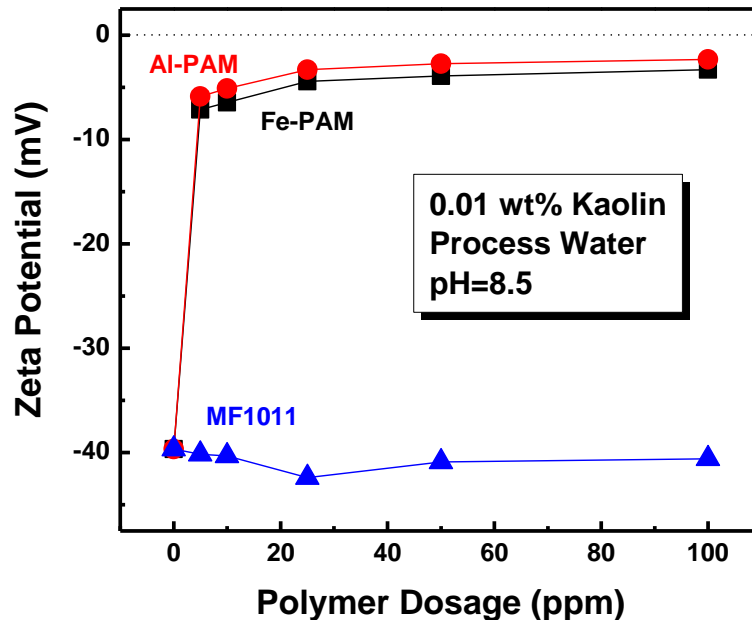


Figure 6-1 Effect of Polymers on Zeta Potential of Kaolin Particles

It is shown in Figure 6-1 that the zeta potentials of kaolin particles become less negative with increasing Al-PAM or Fe-PAM dosage, which indicates the role of electrostatic attractions as a major driving force for the adsorption of cationic hybrids, Al-PAM and Fe-PAM, on negatively charged kaolin particles. The effect

of Al-PAM and Fe-PAM on zeta potential of kaolin was very similar at all dosages tested. At the dosage  $\geq 50$  ppm, both Al-PAM and Fe-PAM were able to increase the zeta potential of kaolin from -40 mV to -5 mV, which reflected the adsorption of positively charged Al-PAM and Fe-PAM molecules on negatively charged kaolin particles, neutralizing negative charges of kaolin particles. No significant increase in zeta potential of kaolin particles was observed when polymer dosage was increased beyond 50 ppm, suggesting that the adsorption of Al-PAM or Fe-PAM at 50 ppm on kaolin particles was almost saturated.

Unlike the cationic hybrids, negatively charged MF 1011 did not show any significant effect on zeta potential of kaolin particles. At 25 ppm, which is the optimum dosage of MF 1011 when flocculating model tailings as mentioned in Chapter 5, a slight decrease in the zeta potential of kaolin particles from -40 mV to -42 mV was observed. This decrease in zeta potential is attributed to the adsorption of anionic MF 1011 through hydrogen bonding mechanism [1].

The results from zeta potential measurement were consistent with the results of flocculation determined by FBRM. The zeta potential of kaolin particles became less negative with increasing Al-PAM or Fe-PAM dosages. The maximum  $d_{50}$  of model tailings increased with increasing Al-PAM and Fe-PAM dosages. MF 1011 exhibited an optimum dosage of 25 ppm from both FBRM and zeta potential measurements. The enhanced flocculation performance of cationic hybrid polymers was attributed to the charge neutralization by their adsorption on kaolin particles.

## 6.2 Adsorption of Polymers on Kaolin Particles

Figure 6-2 shows the amount of polymer adsorbed on kaolin particles as a function of polymer dosage.

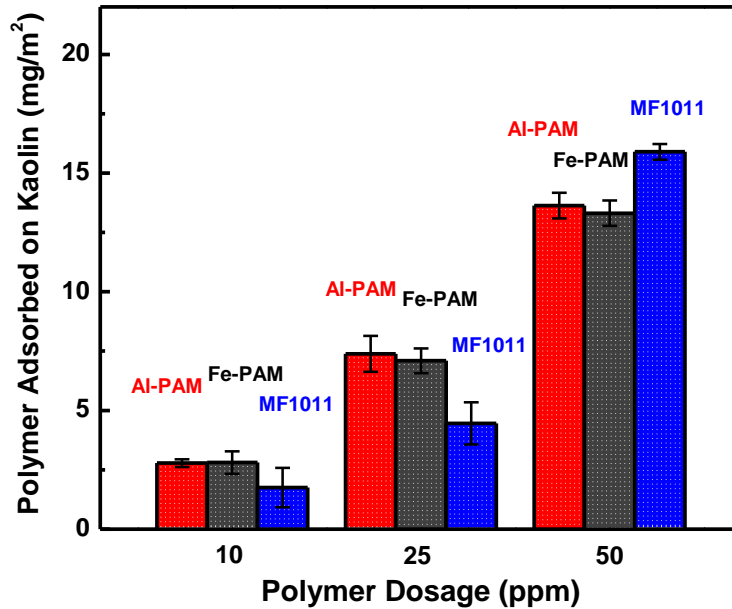


Figure 6-2 Polymer Adsorbed on Kaolin as a Function of Dosage

For Al-PAM and Fe-PAM, around 2.5 mg/m<sup>2</sup>, 7.5 mg/m<sup>2</sup> and 13 mg/m<sup>2</sup> were adsorbed on kaolin particles upon the addition of 10 ppm, 25 ppm and 50 ppm polymer, respectively. For MF 1011, around 1.8 mg/m<sup>2</sup>, 4.5 mg/m<sup>2</sup> and 16 mg/m<sup>2</sup> were adsorbed on kaolin particles upon the addition of 10 ppm, 25 ppm and 50 ppm polymer, respectively. With the addition of 10 ppm and 25 ppm MF 1011, only 1.8 mg/m<sup>2</sup> and 4.5 mg/m<sup>2</sup> polymer was adsorbed on kaolin particles, respectively, because MF 1011 adsorbs on kaolin by hydrogen bonding but hindered by electrostatic repulsion between polymer and clay. At 50 ppm, 16

mg/m<sup>2</sup> MF 1011 adsorbed on kaolin particles, which is more than the amount of Al-PAM or Fe-PAM adsorbed. This is most likely due to the morphology of adsorbed polymers. Because of strong affinity of Al-PAM and Fe-PAM to kaolin particles due to both charge neutralization and hydrogen bonding, they occupy more area per molecules once adsorbed, leading to a less amount that could be adsorbed as compared to MF 1011 at higher dosage.

The TOC results were in good agreement with our FBRM and zeta potential results. Increasing Al-PAM and Fe-PAM dosage led to increased adsorption of polymers by kaolin particles, resulting in less negative surface charge, which facilitated flocculation. Compared with Al-PAM and Fe-PAM, MF 1011 at its optimum dosage of 25 ppm adsorbed less on kaolin. As a result, it was less effective in flocculation of negatively charged kaolin particles. At 50 ppm, excess adsorption of MF 1011 stabilized kaolin particles. Therefore, further increasing MF 1011 dosage to 50 ppm showed adverse effect on flocculation as shown in Figure 5-5.

### **6.3 Summary**

The adsorption of Al-PAM, Fe-PAM and MF 1011 on kaolin was determined by zeta potential and TOC measurement. At  $\geq 50$  ppm, both Al-PAM and Fe-PAM increased the zeta potential of kaolin from -40 mV to -5 mV, which revealed the adsorption of cationic hybrid polymer on negatively charged particles through electrostatic attractions. Continuous increase in polymer dosage beyond 50 ppm did not result in an obvious change in zeta potential of kaolin particles, indicating saturation adsorption at 50 ppm polymer dosage. MF 1011 did not show a

significant effect on zeta potential of kaolin: at 25 ppm, it decreased the zeta potential of kaolin from -40 mV to -42 mV, which is attributed to the adsorption of anionic MF 1011 on kaolin through hydrogen bonding. In TOC measurements, all three polymers showed increased adsorption on kaolin with increasing their dosages. At 10 ppm and 25 ppm, 2.5 mg/m<sup>2</sup> and 7.5 mg/m<sup>2</sup> of Al-PAM and Fe-PAM were adsorbed on kaolin; but only 1.8 mg/m<sup>2</sup> and 4.5 mg/m<sup>2</sup> of MF 1011 were adsorbed on kaolin. This difference in adsorption of Al-PAM and Fe-PAM from MF 1011 on kaolin is attributed to adsorption of Al-PAM and Fe-PAM by both electro-attractive interactions and hydrogen bonding in contrast to MF 1011 which adsorbs by hydrogen bonding, but hindered by electro-repulsive interactions with kaolin particles. At 50 ppm, 13 mg/m<sup>2</sup> of Al-PAM and Fe-PAM were adsorbed on kaolin, in comparison to 16 mg/m<sup>2</sup> for MF 1011. Al-PAM and Fe-PAM adsorbs on kaolin by a synergetic mechanism of electrostatic attraction and hydrogen bonding. As a result, they occupy more area per molecules once adsorbed. So compared with MF 1011, they showed less adsorption at higher dosages. The results were consistent with our flocculation tests: for Al-PAM and Fe-PAM, increasing dosage led to increased adsorption and thus a higher maximum d<sub>50</sub> of flocs. For MF 1011, it showed an optimum dosage at 25 ppm, because higher dosages resulted in an excessive adsorption, which adversely affected its ability of flocculation.

## References

1. Wang, X. W.; Feng, X.; Xu, Z.; Masliyah, J. H. Polymer aids for settling and filtration of oil sands tailings. *The Canadian Journal of Chemical Engineering* **2010**, 88 (3), 403-410.

## Chapter 7 Flocculation of Laboratory Extraction Tailings

### 7.1 Effect of Al-PAM on Flocculation

Figure 7-1 shows the effect of Al-PAM on maximum  $d_{50}$  of laboratory extraction tailings. With the addition of 25 ppm, 50 ppm and 75 ppm of Al-PAM, the maximum  $d_{50}$  of laboratory extraction tailings increased from  $\sim 30 \mu\text{m}$  to  $\sim 35 \mu\text{m}$ ,  $60 \mu\text{m}$  and  $85 \mu\text{m}$ , respectively. It is clearly shown that at dosages lower than 100 ppm, Al-PAM did not significantly increase the maximum  $d_{50}$  of laboratory extraction tailings. At 100 ppm, the maximum  $d_{50}$  of flocs was  $\sim 300 \mu\text{m}$ . Higher dosage of Al-PAM led to better flocculation measured in terms of maximum  $d_{50}$  of flocs, which might be attributed to more surface coverage of solids by Al-PAM.

Figure 7-2 shows the comparison between the effects of Al-PAM on model and laboratory extraction tailings. It is clearly shown that Al-PAM was more effective in flocculating model tailings than laboratory extraction tailings. At 25 ppm and 50 ppm, for example, it increased the maximum  $d_{50}$  of model tailings from  $20.9 \mu\text{m}$  to  $529 \mu\text{m}$  and  $616 \mu\text{m}$ , respectively. In contrast, at the same dosages, Al-PAM increased the maximum  $d_{50}$  of laboratory extraction tailings from  $\sim 30 \mu\text{m}$  only to  $35 \mu\text{m}$  and  $60 \mu\text{m}$ , respectively. Such different results may be attributed to two reasons: first, the solids concentration of laboratory extraction tailings (15.3% by weight) is three times as much as that of model tailings (5% by weight); secondly, laboratory extraction tailings also contain residual bitumen that polymer

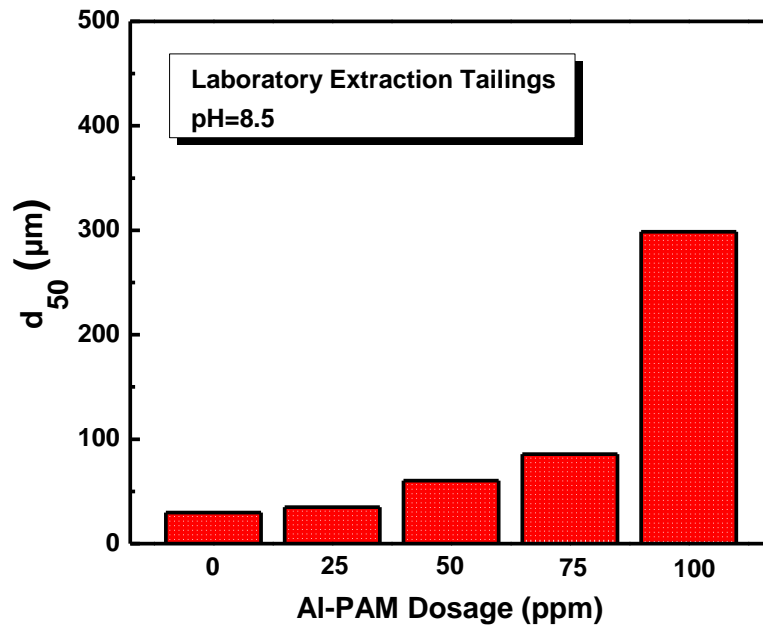


Figure 7-1 Effect of Al-PAM Dosage on Maximum  $d_{50}$  of Laboratory Extraction Tailings

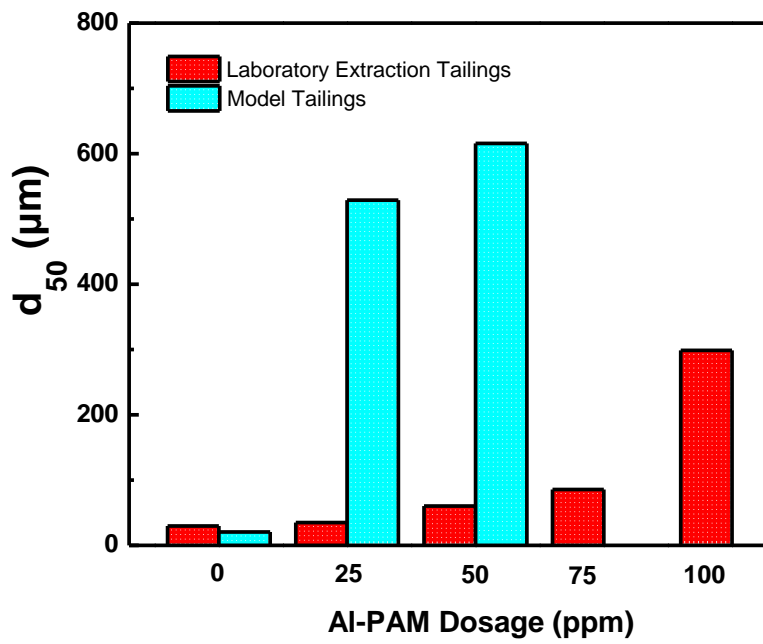


Figure 7-2 Comparison between Effect of Al-PAM on Model Tailings and Laboratory Extraction Tailings

would adsorb on. Therefore, at the same dosage, the effect of Al-PAM on model tailings was more significant than that on laboratory extraction tailings.

### 7.2 Effect of Fe-PAM on Flocculation

As shown in Figure 7-3, the effect of Fe-PAM on flocculation of laboratory extraction tailings exhibits the same trend as that of Al-PAM. At 25 ppm, 50 ppm and 75 ppm, Fe-PAM increased the maximum  $d_{50}$  of laboratory extraction tailings from  $\sim 30 \mu\text{m}$  to  $\sim 40 \mu\text{m}$ ,  $60 \mu\text{m}$  and  $90 \mu\text{m}$ , respectively. At 100 ppm, the maximum  $d_{50}$  of induced flocs was around  $350 \mu\text{m}$ . With increasing polymer

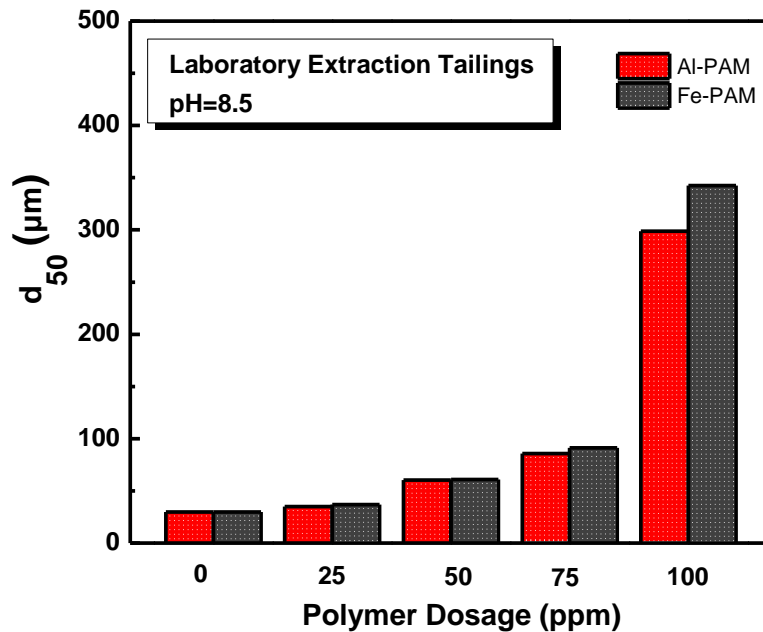


Figure 7-3 Effect of Fe-PAM Dosage on Maximum  $d_{50}$  of Laboratory Extraction Tailings

dosage, more Fe-PAM adsorbed on solids, resulting in larger flocs.

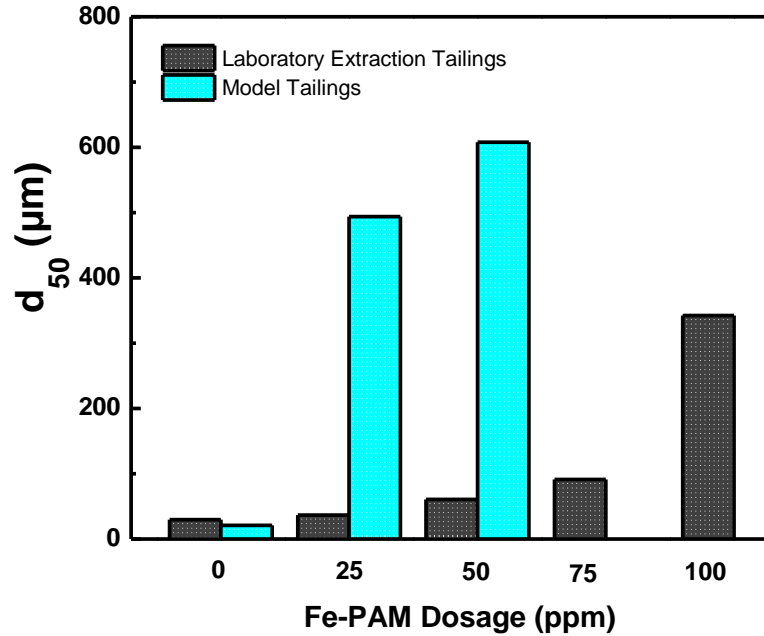


Figure 7-4 Comparison between Effect of Fe-PAM on Model Tailings and Laboratory Extraction Tailings

Similar to that of Al-PAM, the effect of Fe-PAM on model tailings was more obvious than that on laboratory extraction tailings. As shown in Figure 7-4, at 25 ppm and 50 ppm, Fe-PAM increased the maximum  $d_{50}$  of model tailings from 20.9  $\mu\text{m}$  to 494  $\mu\text{m}$  and 608  $\mu\text{m}$ , respectively. However, at the same dosages, it increased the maximum  $d_{50}$  of laboratory extraction tailings from ~30  $\mu\text{m}$  only to 40  $\mu\text{m}$  and 60  $\mu\text{m}$ , respectively. Laboratory extraction tailings contain 15.3 wt% of solids and 1.6 wt% of bitumen, but model tailings contain only 5 wt% of solids. The different composition of model and laboratory extraction tailings led to distinct effectiveness of Fe-PAM on them.

### 7.3 Effect of MF 1011 on Flocculation

In contrast to Al-PAM or Fe-PAM, MF 1011 at higher dosages (> 25 ppm) did not show remarkable effect on maximum  $d_{50}$  of laboratory extraction tailings. As shown in Figure 7-5, at 50 ppm, 75 ppm and 100 ppm, MF 1011 increased the maximum  $d_{50}$  of laboratory extraction tailings from ~30  $\mu\text{m}$  to 90  $\mu\text{m}$ , 40  $\mu\text{m}$  and 50  $\mu\text{m}$ , respectively. At its optimum dosage, 25 ppm, MF 1011 increased the maximum  $d_{50}$  of laboratory extraction tailings from ~30  $\mu\text{m}$  to 100  $\mu\text{m}$ . MF 1011 was found sensitive to overdose in flocculation of both model and laboratory extraction tailings [1].

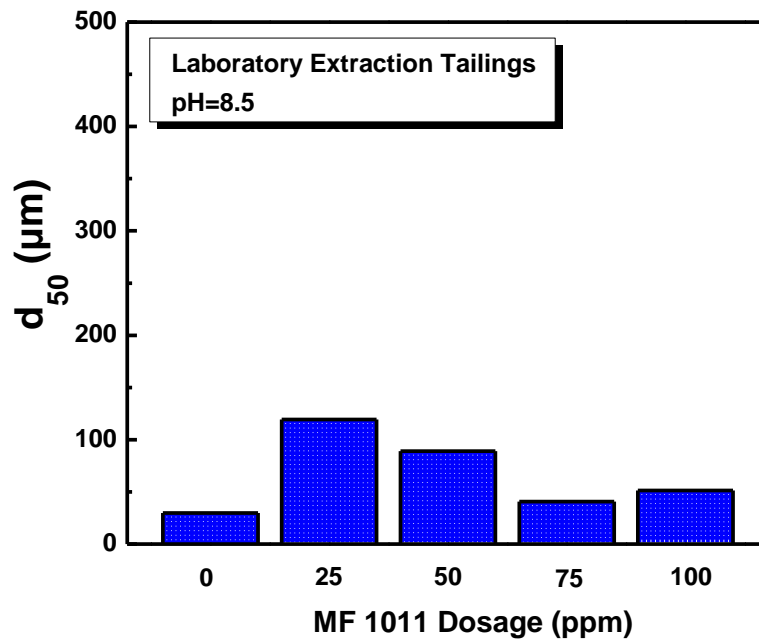


Figure 7-5 Effect of MF 1011 Dosage on Maximum  $d_{50}$  of Laboratory Extraction Tailings

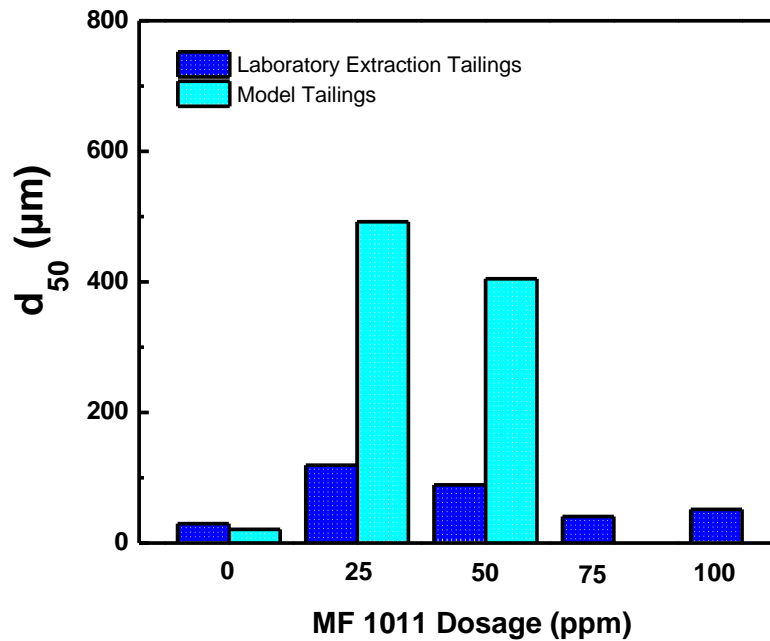


Figure 7-6 Comparison between Effect of MF 1011 on Model Tailings and Laboratory Extraction Tailings

The effect of MF 1011 on model and laboratory extraction tailings was shown in Figure 7-6. At 25 ppm and 50 ppm, MF 1011 increased the maximum  $d_{50}$  of model tailings from 20.9  $\mu\text{m}$  to 492  $\mu\text{m}$  and 425  $\mu\text{m}$ , respectively. In contrast, at the same dosages, it increased the maximum  $d_{50}$  of laboratory extraction tailings from ~30  $\mu\text{m}$  to 100  $\mu\text{m}$  and 90  $\mu\text{m}$ , respectively. MF 1011 was shown to be more effective in flocculation of model tailings than laboratory extraction tailings, as model tailings contain less solids (5 wt%, compared to 15.3 wt% in laboratory extraction tailings) and no bitumen.

#### **7.4 Comparison among Al-PAM, Fe-PAM and MF 1011**

As shown in Figure 7-7, addition of either Al-PAM or Fe-PAM at low dosages (<100 ppm) did not show any significant effect on maximum  $d_{50}$  of laboratory extraction tailings. However, the effect of polymer on maximum  $d_{50}$  of laboratory extraction tailings became dramatic when its dosage increased to 100 ppm. It is clearly shown in Figure 7-7 that the maximum  $d_{50}$  of particles in laboratory extraction tailings increased from 30  $\mu\text{m}$  to 300  $\mu\text{m}$  and 350  $\mu\text{m}$ , after addition of 100 ppm Al-PAM and Fe-PAM, respectively. Larger flocs were formed with the addition of Fe-PAM compared to Al-PAM, which might be ascribed to the higher affinity of Fe-PAM to residual bitumen that remains in laboratory extraction tailings. Therefore Fe-PAM might facilitate the hetero-coagulation of fines and bitumen droplets, leading to the formation of larger flocs.

On the other hand, MF 1011 showed an optimum dosage of 25 ppm with a corresponding maximum  $d_{50}$  value of 100  $\mu\text{m}$ . This value is much smaller than the maximum  $d_{50}$  obtained after the addition of either Al-PAM or Fe-PAM at 100 ppm. The result shows that Al-PAM or Fe-PAM could be a better choice than MF 1011 in flocculation of laboratory extraction tailings at higher dosages. However, at lower dosages (<100 ppm), Al-PAM and Fe-PAM were less effective than MF 1011, which might be due to their lower molecular weights than MF 1011.

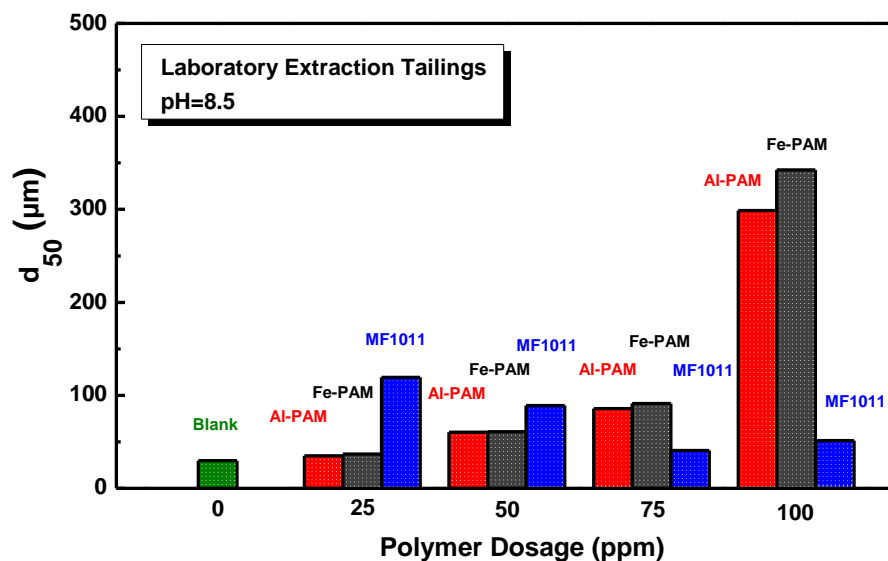


Figure 7-7 Comparison among Al-PAM, Fe-PAM and MF 1011

### 7.5 Strength of Floccs Formed by Different Polymers

To compare the strength of floccs induced by different polymers at their optimum dosages, the evolution of  $d_{50}$  of laboratory extraction tailings was recorded as a function of stirring time. Al-PAM, Fe-PAM and MF 1011 at 100 ppm, 100 ppm and 25 ppm, respectively, were added to laboratory extraction tailings stirred at 650 rpm. Results are shown in Figure 7-8. It was found that upon addition of Al-PAM or Fe-PAM, the  $d_{50}$  of particles in laboratory extraction tailings increased to maximum value (~350  $\mu\text{m}$  and 425  $\mu\text{m}$ , respectively), but decreased afterwards during the measurement. This observation suggested that the shearing forces at the stirring rate of 650 rpm could either break the floccs induced by hybrid polymers or make the floccs more compact. However, after addition of MF 1011, the  $d_{50}$  of particles in laboratory extraction tailings reached the optimum value

(125  $\mu\text{m}$ ) and then remained stable, indicating that the flocs formed were sufficiently strong to endure the high shear rate used [2].

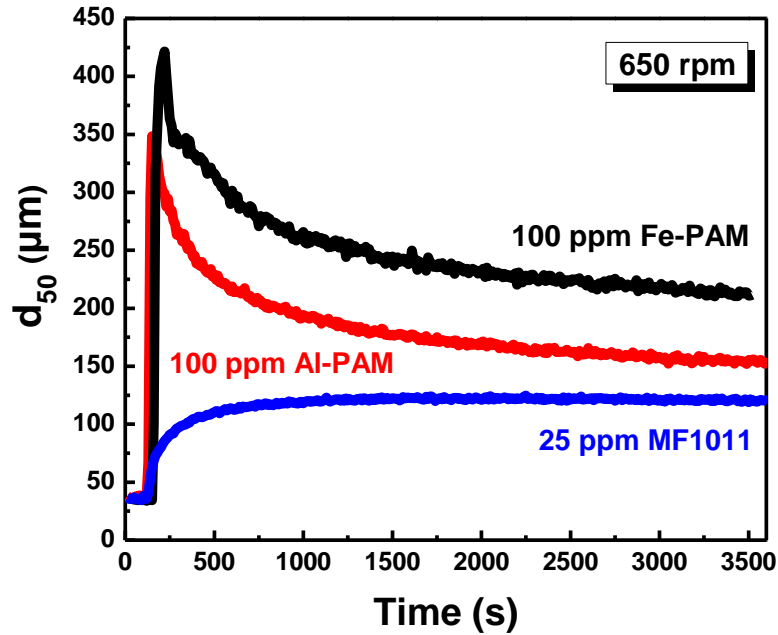


Figure 7-8  $d_{50}$  of Laboratory Extraction Tailings with Polymer Addition as a Function of Time

The results obtained from FBRM tests were further confirmed by experiments on ISR of laboratory extraction tailings at extended mixing time. Results of ISR experiments are presented in Figure 7-9. It is clearly shown that when the stirring time (after Al-PAM or Fe-PAM addition) increased from 0 to 5 minutes, the ISR of tailings slurry dropped from 80 m/h to 35 m/h. However, when laboratory extraction tailings was flocculated by MF 1011 and then agitated for 5 minutes, the ISR remained constant. One explanation could be related to structure of the flocs formed by three different polymers. The flocs induced by MF 1011 had

smaller size while trapped a large amount of water (open structure flocs). Thus, when using high shear rate, the mechanical energy is dissipated within the flocs and made them more resistant to shear within the range studied [3]. On the other hand, flocs formed by Al-PAM or Fe-PAM were larger in size and rigid. This type of flocs could easily break under the high shear used. Therefore, the floc size and ISR of laboratory extraction tailings flocculated by Al-PAM or Fe-PAM decreased with extended mixing time at 650 rpm.

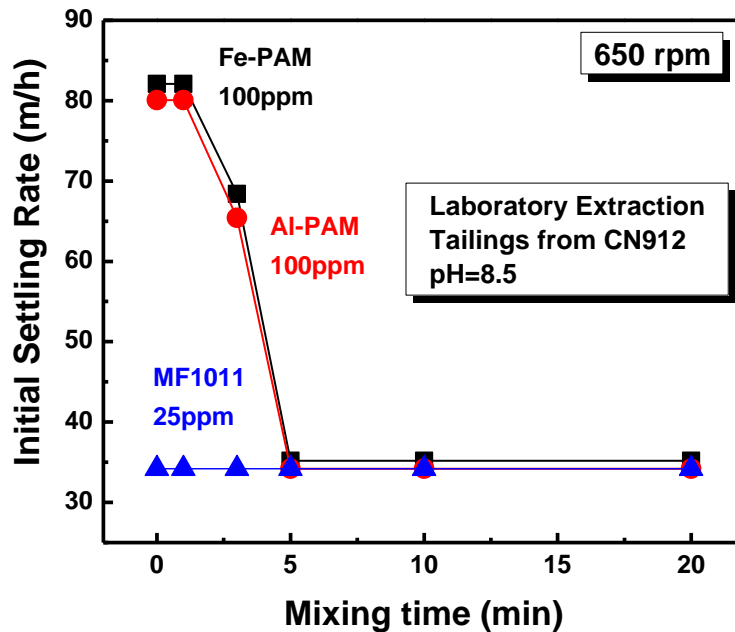


Figure 7-9 Initial Settling Rate of Laboratory Extraction Tailings at Extended Mixing Time

## 7.6 Summary

Al-PAM, Fe-PAM and MF 1011 were used in flocculation of laboratory extraction tailings. For hybrid polymers at dosages less than 100 ppm, they did not show any significant effect on the maximum  $d_{50}$  of laboratory extraction tailings. However, at 100 ppm, Al-PAM and Fe-PAM increased the maximum  $d_{50}$  of laboratory extraction tailings from  $\sim 30 \mu\text{m}$  to  $300 \mu\text{m}$  and  $350 \mu\text{m}$ , respectively. MF 1011 showed an optimum dosage of 25 ppm, at which it increased the maximum  $d_{50}$  of laboratory extraction tailings from  $\sim 30 \mu\text{m}$  to  $100 \mu\text{m}$ . Compared with model tailings, Al-PAM, Fe-PAM and MF 1011 were less effective in flocculation of laboratory extraction tailings, as laboratory extraction tailings not only contain more solids but also contain residual bitumen that could consume more polymer. The flocs formed by MF 1011 at 25 ppm were resistant to the shear forces under the shear rate of 650 rpm, but the flocs formed with 100 ppm Al-PAM or Fe-PAM were broken under the same shear rate, as indicated by a decrease in maximum  $d_{50}$  of flocs and in ISR of laboratory extraction tailings at a prolonged stirring time.

## References

1. Li, H.; Long, J.; Xu, Z.; Masliyah, J. H. Synergetic role of polymer flocculant in low-temperature bitumen extraction and tailings treatment. *Energy & Fuels* **2005**, *19* (3), 936-943.
2. Alfano, J. C.; Carter, P. W.; Dunham, A. J.; Nowak, M. J.; Tubergen, K. R. Polyelectrolyte-induced aggregation of microcrystalline cellulose:

Reversibility and shear effects. *Journal of Colloid and Interface Science* **2000**, 223 (2), 244-254.

3. Tokita, M.; Nishinari, K., Gels: Structures, Properties and Functions. In *Progress in Colloid and Polymer Science*, Springer: 2009; Vol. 136.

## **Chapter 8 Adsorption of Polymers on Oil Sands Components**

To study the interactions between polymers and oil sands tailings components, the zeta potentials of fines in laboratory extraction tailings and bitumen with polymers addition at their optimum dosages for flocculation were measured.

### **8.1 Interactions of Polymers with Fines in Laboratory Extraction Tailings**

The interactions of polymers with fines in laboratory extraction tailings were studied by zeta potential measurements. Al-PAM, Fe-PAM and MF 1011 were added to fine solid suspensions at 100 ppm, 100 ppm and 25 ppm, respectively. It is clearly shown in Figure 8-1 that addition of 100 ppm Al-PAM or Fe-PAM significantly increased the zeta potential of fines in laboratory extraction tailings from -20 mV to -6 mV and -8 mV, respectively. The significant decrease in zeta potential reflected the adsorption of positively charged Al-PAM and Fe-PAM on negatively charged fine particles, neutralizing negative charges of fine particles. In the case of MF 1011 at optimal dosage of 25 ppm, the zeta potential of fine particles decreased from -20 mV to -22 mV. The change in zeta potential is less than that caused by Al-PAM or Fe-PAM due to the anionic nature of MF 1011. The major driving forces for adsorption in MF 1011 case is hydrogen bonding between MF 1011 and fines [1]. The zeta potential results are consistent with previous FBRM results: at 100 ppm, Al-PAM and Fe-PAM adsorbed on solid surfaces by both electrostatic attraction and hydrogen bonding, which led to the

formation of larger and denser flocs and thus better flocculation performance than MF 1011.

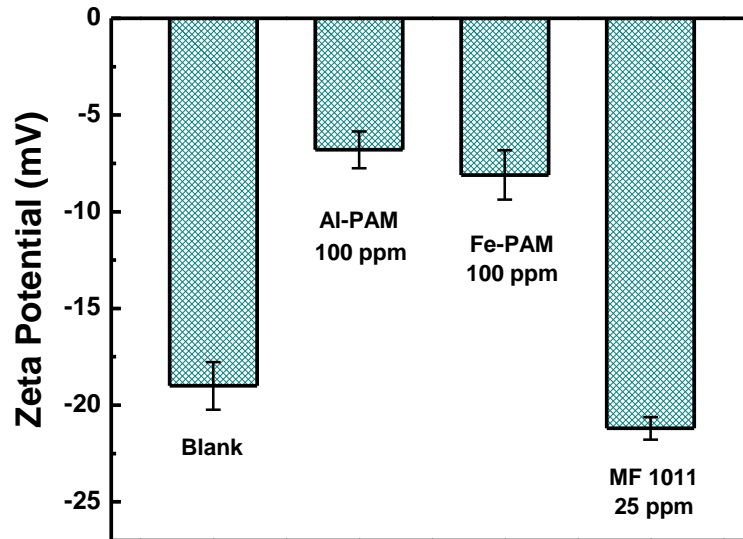
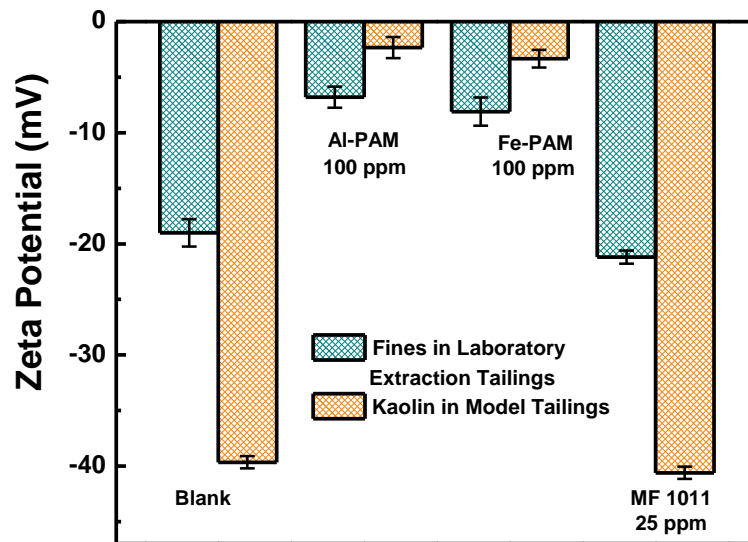


Figure 8-1 Effect of Polymers on Surface Charge of Fines



## Figure 8-2 Comparison between Effect of Polymers on Surface Charge of Fines in Laboratory Extraction Tailings and Kaolin in Model Tailings

Figure 8-2 shows the comparison between effect of polymers on fines in laboratory extraction tailings and kaolin in model tailings. Upon addition of 100 ppm Al-PAM or Fe-PAM, the zeta potential of fines in laboratory extraction tailings increased from -20 mV to -6 mV and -8 mV, respectively. At the same dosage, the zeta potential of kaolin in model tailings increased from -40 mV to -2 mV and -3 mV, respectively. The significant increase in zeta potential of solids reflected the adsorption of cationic polymers on negatively charged fines or kaolin particles through electrostatic attraction. Moreover, at the same dosage, hybrid polymers were found to be more effective on neutralizing surface charge of kaolin than that of fines in laboratory extraction tailings. In contrast, with 25 ppm MF 1011 (the optimum dosage in flocculation of both model and laboratory extraction tailings), the zeta potential of fines in laboratory extraction tailings and kaolin in model tailings decreased from -20 mV to -22 mV and from -40 mV to -42 mV, respectively. The decrease in zeta potential is attributed to the adsorption of anionic MF 1011 through hydrogen bonding mechanism.

### **8.2 Interactions of Polymers with Bitumen**

Since the laboratory extraction tailings from CN912 contain 1.6 wt% of bitumen, the interactions of polymers with bitumen were also investigated. It is shown in Figure 8-3 that the zeta potential of bitumen increased from -52 mV to -25 mV and -22 mV, after addition of 100 ppm Al-PAM and Fe-PAM, respectively, which

indicates strong adsorption of Al-PAM and Fe-PAM on bitumen. MF 1011 was also adsorbed on bitumen surface, as the zeta potential of bitumen became less negative (from -52 mV to -61 mV) with 25 ppm MF 1011. This finding suggests that Fe-PAM have more affinity to bitumen than Al-PAM, thus in the case of laboratory extraction tailings, Fe-PAM showed better performance than Al-PAM at optimum dosage. To confirm this hypothesis, further study on adsorption of polymers on simulated clays and bitumen surfaces (major components in oil sands ore) was investigated and will be shown in the following section.

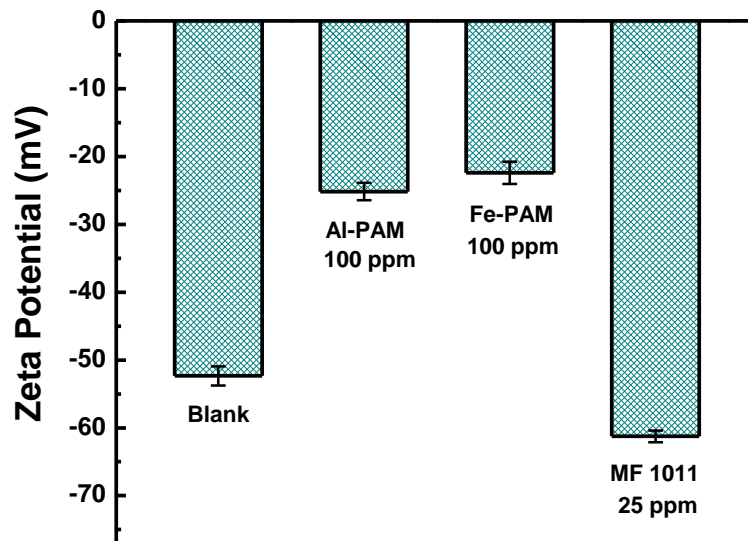


Figure 8-3 Effect of Polymers on Surface Charge of Bitumen

### 8.3 Adsorption of Polymers on Silica (Simulating Silica Basal Planes)

Adsorption kinetics of Al-PAM, Fe-PAM and MF 1011 on silica in filtered process water are shown in Figure 8-4. It is obvious that Al-PAM and Fe-PAM

have very similar adsorption profiles. After switching the background solution to 100 ppm polymer solution, both Al-PAM and Fe-PAM exhibited rapid adsorption and reached equilibrium very quickly. Further rinsing with filtered process water did not result in any desorption, which indicates a stable and irreversible adsorption. At equilibrium, both Al-PAM and Fe-PAM adsorbed  $5.5 \text{ mg/m}^2$  on silica. The fast and strong adsorption is due to the electrostatic attractive interactions between negatively charged silica surface and positively charged  $\text{Al(OH)}_3$  or  $\text{Fe(OH)}_3$  colloidal particles in Al-PAM or Fe-PAM molecular structures [2]. MF 1011 shows negligible adsorption on silica due to repulsive forces between negatively charged silica surface and anionic moieties in MF1011. These results are in good agreement with a previous study of polymers adsorption on silica surface in Milli-Q water [2].

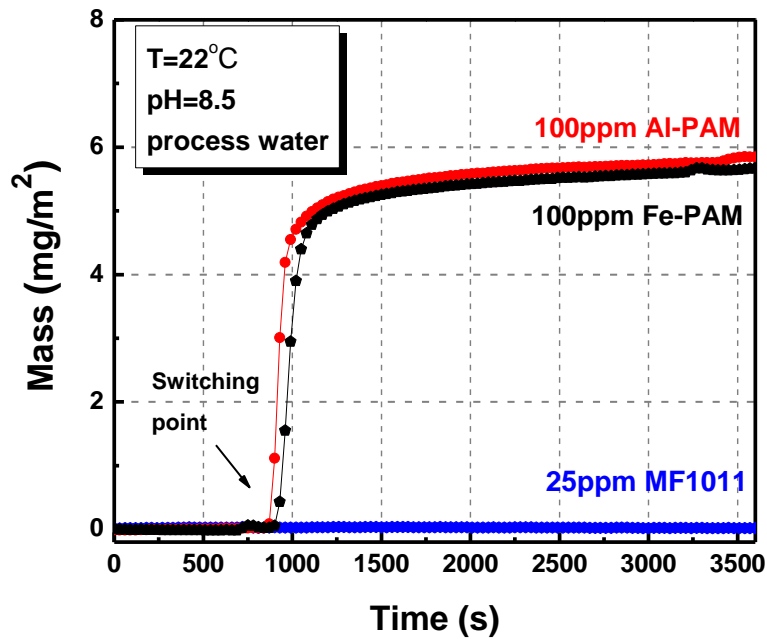


Figure 8-4 Adsorption of Polymers on Silica

#### 8.4 Adsorption of Polymers on Alumina (Simulating Alumina Basal Planes)

Adsorption characteristics of Al-PAM, Fe-PAM and MF1011 at pH 8.5 on alumina are shown in Figure 8-5. Compared with the two hybrid polymers, MF 1011 showed the highest adsorption. At equilibrium, the adsorbed mass of MF 1011 is  $\sim 4.5 \text{ mg/m}^2$  as compared to  $3.5 \text{ mg/m}^2$  in the case of both Al-PAM and Fe-PAM. One explanation is that at pH 8.5, MF 1011 adsorbed on alumina through both attractive electrostatic interactions between anionic MF 1011 molecules and positively charged alumina surface and through hydrogen bonding, leading to fast and strong adsorption. On the other hand, cationic hybrid polymers experience some repulsive interaction with alumina surface due to their cationic nature and adsorbed on alumina surface only by hydrogen bonding [2].

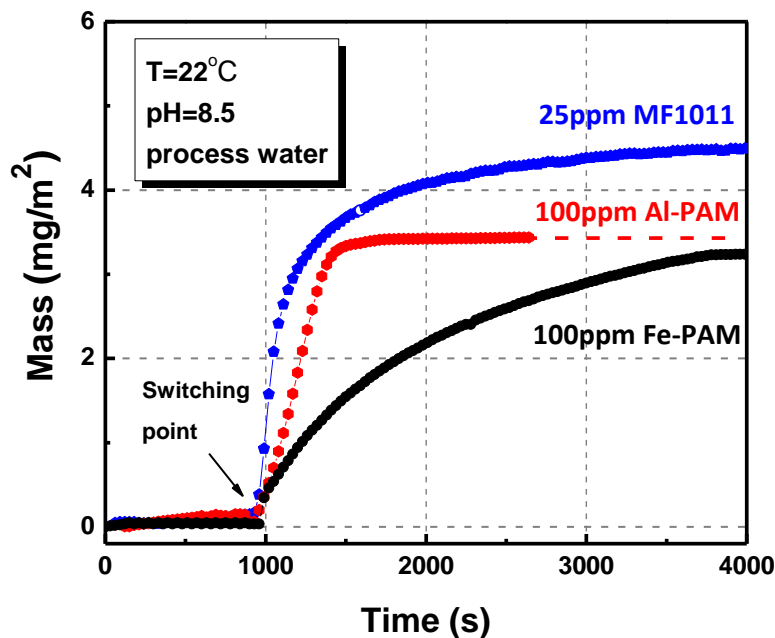


Figure 8-5 Adsorption of Polymers on Alumina

It is interesting to note that the adsorption of Al-PAM on alumina is faster than that of Fe-PAM, but the equilibrium mass of Al-PAM and Fe-PAM adsorbed on alumina is similar.

### 8.5 Adsorption of Polymers on Bitumen

The adsorption kinetics of three polymers on bitumen surfaces are shown in Figure 8-6. Compared with their adsorptions on silica and alumina, Al-PAM, Fe-PAM and MF 1011 exhibited slower and weaker adsorption on bitumen. The equilibrium masses of Al-PAM, Fe-PAM and MF 1011 adsorbed on bitumen are  $1.7 \text{ mg/m}^2$ ,  $2.5 \text{ mg/m}^2$  and  $1 \text{ mg/m}^2$ , respectively. For negatively charged hydrophobic bitumen surface, cationic Al-PAM and Fe-PAM exhibited a stronger adsorption than anionic MF 1011. Moreover, Fe-PAM adsorbed more than

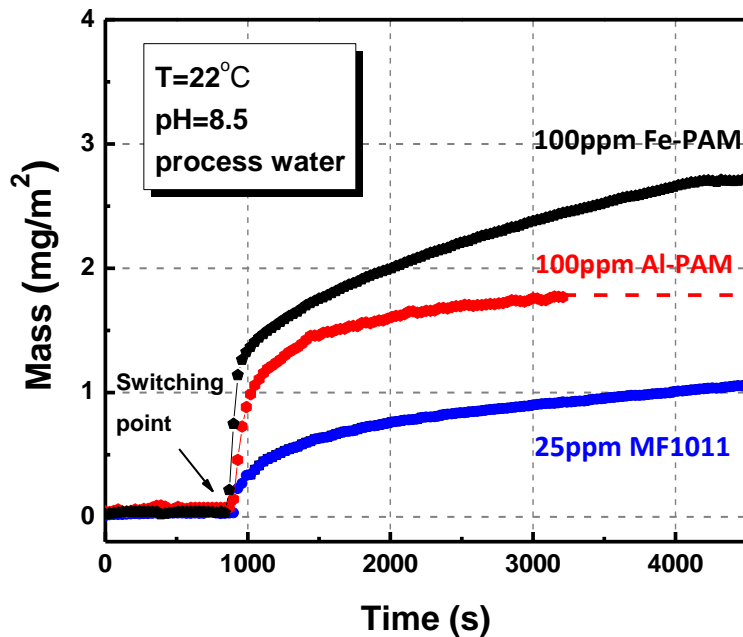


Figure 8-6 Adsorption of Polymers on Bitumen

Al-PAM did, which confirmed the previously mentioned hypothesis that Fe-PAM has a stronger affinity to bitumen than Al-PAM does. Results obtained are consistent with FBRM results: for laboratory extraction tailings containing 1.6 wt% of bitumen, Fe-PAM was more effective than Al-PAM in flocculation.

### 8.6 Comparison among Equilibrium Mass of Polymers Adsorbed on Different Surfaces

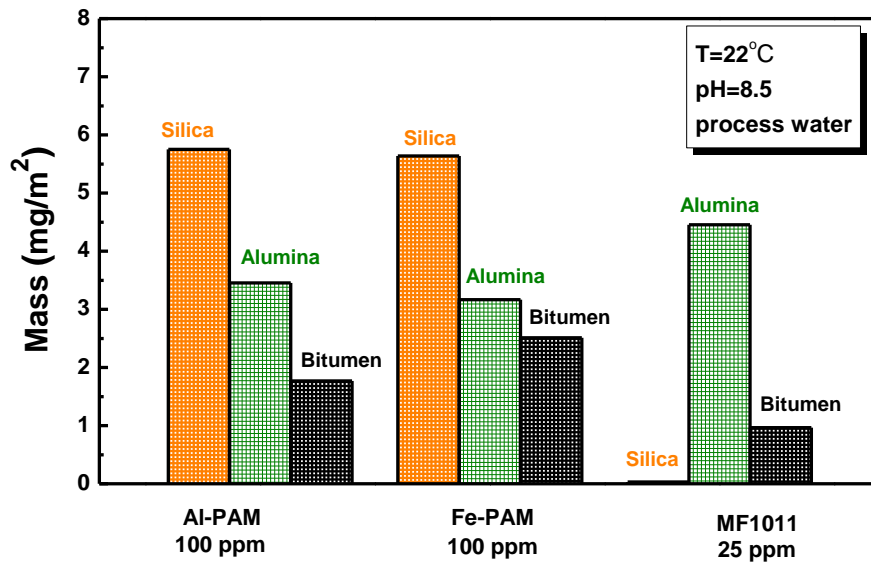


Figure 8-7 Comparison among Equilibrium Mass of Polymers Adsorbed on Different Surfaces

Figure 8-7 shows the equilibrium masses of three polymers, Al-PAM, Fe-PAM and MF 1011 adsorbed on different surfaces in filtered process water at pH 8.5. At 100 ppm, both Al-PAM and Fe-PAM adsorbed in similar manner with a total adsorbed mass of  $5.5 \text{ mg/m}^2$  on silica and  $3.5 \text{ mg/m}^2$  on alumina at equilibrium. The difference between the masses adsorbed on silica and alumina surfaces was caused by surface charges. At pH 8.5, the silica surface is negatively charged while the alumina surface is slightly positive, therefore more mass uptake from cationic polymers solution was observed on silica. Since MF 1011 carried negative charge, it showed negligible adsorption on silica and the most adsorption on alumina surface among the three polymers. On negatively charged bitumen surfaces, cationic Al-PAM and Fe-PAM adsorbed better than anionic MF 1011. Cationic hybrid polymers were preferentially adsorbed on negatively charged model silica than on alumina basal planes and bitumen surface, indicating critical role of surface charges in polymer adsorption and hence their flocculation.

### **8.7 Summary**

The adsorption of Al-PAM, Fe-PAM and MF 1011 on oil sands components was determined by zeta potential measurements and QCM-D tests. With 100 ppm Al-PAM and Fe-PAM, the zeta potential of fines in laboratory extraction tailings increased from -20 mV to -6 mV and -8 mV, respectively, indicating their strong adsorption on negatively charged fines in laboratory extraction tailings. MF 1011 at 25 ppm only decreased the zeta potential of fines from -20 mV to -22 mV due to the anionic nature of MF 1011. The major driving force for the adsorption of MF 1011 is hydrogen bonding between MF 1011 and fines. Compared with

kaolin in model tailings, hybrid polymers were found to be less effective in neutralizing the surface charge of fines in laboratory extraction tailings than kaolin in modeling tailings. Hybrid polymers also showed strong adsorption on bitumen: at 100 ppm, Al-PAM and Fe-PAM increased the zeta potential of bitumen from -52 mV to -25 mV and -22 mV, respectively. MF 1011 was also adsorbed on bitumen surface, as the zeta potential of bitumen became more negative (from -52 mV to -61 mV) with 25 ppm MF 1011 addition.

The adsorption profile of polymers on silica, alumina and bitumen was obtained with QCM-D. At 100 ppm, both Al-PAM and Fe-PAM adsorbed in similar manner with a total adsorbed mass at equilibrium of  $5.5 \text{ mg/m}^2$  on silica and  $3.5 \text{ mg/m}^2$  on alumina. The difference between the masses adsorbed on silica and alumina surfaces was caused by surface charges. At pH 8.5, the silica surface is negatively charged while the alumina surface is slightly positive. As a result, more mass uptake from cationic polymers solution was observed on negatively charged silica than on positively charged alumina surfaces. Since MF 1011 carried negative charge, it showed negligible adsorption on silica and the most adsorption on alumina surface among the three polymers. On negatively charged bitumen surfaces, cationic Al-PAM and Fe-PAM adsorbed better than anionic MF 1011. Cationic hybrid polymers were preferentially adsorbed on model silica than on alumina basal planes and bitumen surface, indicating critical role of surface charges in polymer adsorption.

## References

1. Masliyah, J. H., *Fundamentals of oil sands extraction: CHE534 Course Pack*. 2009.
2. Alagha, L.; Wang, S.; Xu, Z.; Masliyah, J. Adsorption Kinetics of a Novel Organic–Inorganic Hybrid Polymer on Silica and Alumina Studied by Quartz Crystal Microbalance. *The Journal of Physical Chemistry C* **2011**, *115* (31), 15390-15402.

## Chapter 9 Conclusions

To understand the role of cationic inorganic-organic hybrid polymers, Al-PAM and Fe-PAM as novel flocculants in oil sands tailings treatment, the flocculation dynamics of model and laboratory extraction tailings were investigated with FBRM, and the adsorption kinetics of polymers on oil sands components were determined by QCM-D. Al-PAM and Fe-PAM are more effective in flocculating both model and laboratory extraction tailings than MF 1011 at higher dosages. The better performance of Al-PAM and Fe-PAM could be attributed to their charge neutralization and hydrogen bonding mechanisms in adsorption on particles in tailings. Zeta potential measurements confirmed their adsorption on solids. QCM-D results revealed the rapid and strong adsorption of Al-PAM and Fe-PAM on oil sands components, and the strong affinity of Fe-PAM to bitumen. Therefore, Fe-PAM showed better performance than Al-PAM with the presence of bitumen in tailings.

The followings are the major findings of the work:

1. Al-PAM and Fe-PAM were effective in flocculation of both model and laboratory extraction tailings. The maximum  $d_{50}$  of flocs increased with increasing polymer dosage. At polymer dosages beyond 50 ppm for model tailings and 100 ppm for laboratory extraction tailings, flocs with sizes greater than 1000  $\mu\text{m}$  were formed, which exceeded the measurement

range of FBRM. MF 1011 exhibited an optimum dosage at 25 ppm and overdose effect.

2. The maximum  $d_{50}$  of flocs was strongly affected by mixing method and stirring rate. With baffle, the maximum  $d_{50}$  of flocs formed with three polymers decreased by 100  $\mu\text{m}$ . Increasing stirring rate from 400 rpm to 650 rpm led to a decrease in maximum  $d_{50}$  of flocs by 200  $\mu\text{m}$ .
3. Al-PAM, Fe-PAM and MF 1011 were more effective in flocculation of model tailings than laboratory extraction tailings. This difference is attributed to the fact that laboratory extraction tailings not only contains more solids but also have residual bitumen which consumes polymer.
4. Al-PAM and Fe-PAM adsorbed on solids by a synergetic mechanism of charge neutralization and hydrogen bonding. In contrast, MF 1011 adsorbed on negatively charged solids or bitumen only by hydrogen bonding and hindered by electrostatic repulsive forces between MF 1011 and solids or bitumen.
5. Zeta potential and QCM-D measurement results showed that Fe-PAM had a stronger affinity to bitumen than Al-PAM. With the presence of bitumen in tailings slurry, Fe-PAM could be a better flocculant.

## Chapter 10 Recommendations for Future Research

This work mainly focused on flocculation of model and laboratory extraction tailings by hybrid polymers Al-PAM and Fe-PAM at room temperature. However, real tailings from extraction plant or tailings pond may have higher or lower temperature and more complicated compositions. Such differences may affect the flocculation and polymer adsorption. Besides, residual polymer in tailings water may have some impacts on bitumen recovery when it recycled to extraction process, as Al-PAM and Fe-PAM would also adsorb on bitumen. To better understand the role of inorganic-organic hybrid polymers in oil sands tailings treatment, the interaction forces between clays, sands and bitumen with addition of each polymer should be measured. Therefore, the recommendations for future research on flocculation of oil sands tailings by inorganic-organic hybrid polymers are listed as follows:

- 1) Study the flocculation and adsorption processes at different temperatures;
- 2) Test the adaptability of Al-PAM and Fe-PAM on various real tailings;
- 3) Study the effect of residual polymer in tailings water on bitumen extraction;
- 4) Measure the interaction forces between clays, sands and bitumen with polymers at various dosages.